Ultra-low Power/Energy Efficient High Accuracy CMOS Temperature Sensors for passive RFID Applications

Prof. Man-Kay Law

Institute of Microelectronics
State Key Laboratory of
Analog and Mixed-Signal VLSI
(University of Macau)
微電子研究院
漠擬與混合信號超大規模集成電路
國家重點實驗室（澳門大學）

澳門大學
UNIVERSIDADE DE MACAU
UNIVERSITY OF MACAU

IME
SKL AMSV

Outline

- Motivation and Challenge
- Fundamentals of BJT-based CMOS Temperature Sensing
- Design Examples
  - Ultra-low Power High Accuracy CMOS Temperature Sensor for Clinical Temperature Monitoring
  - Embedded Time-Domain Wide Sensing Range CMOS Temperature Sensor
- Conclusions

Emerging Sensing/Biomedical Applications

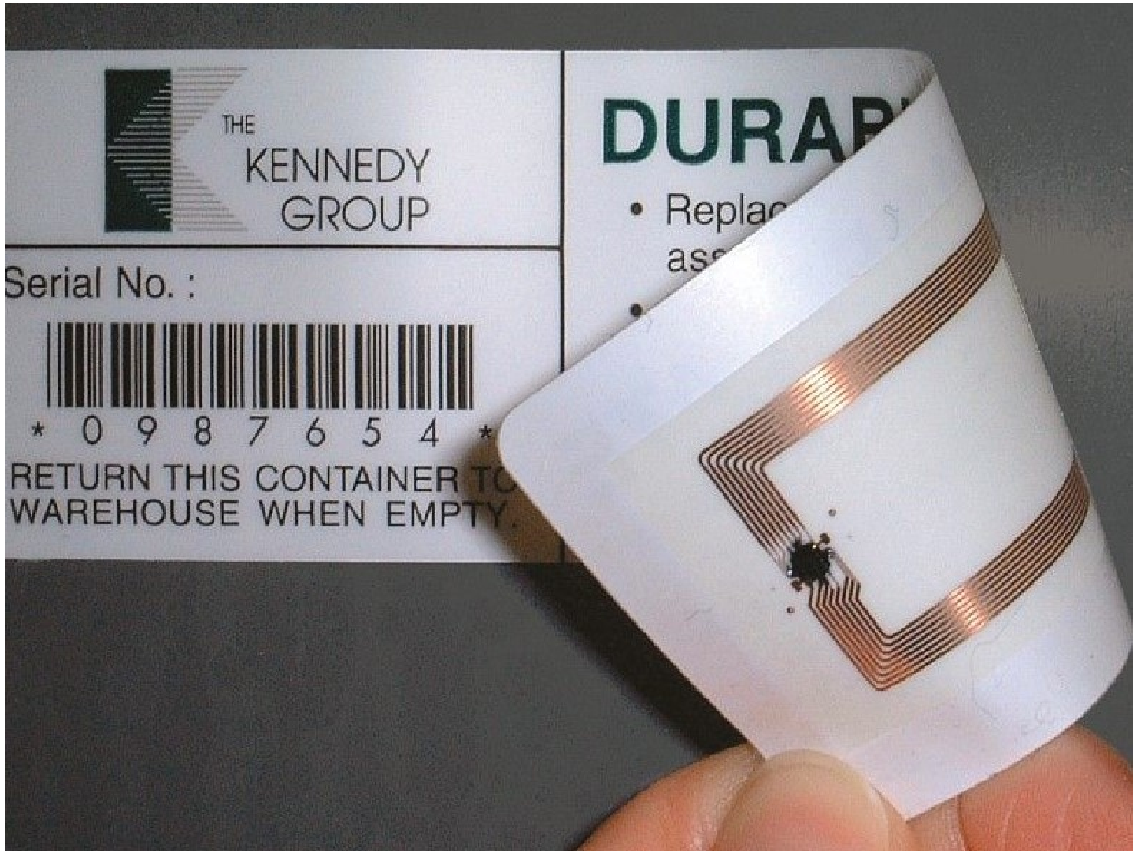

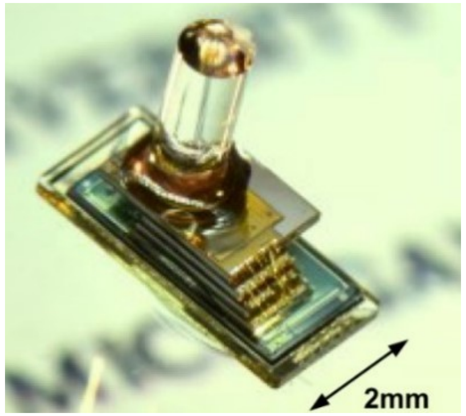

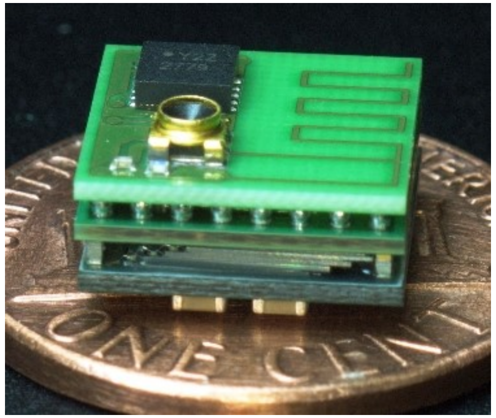

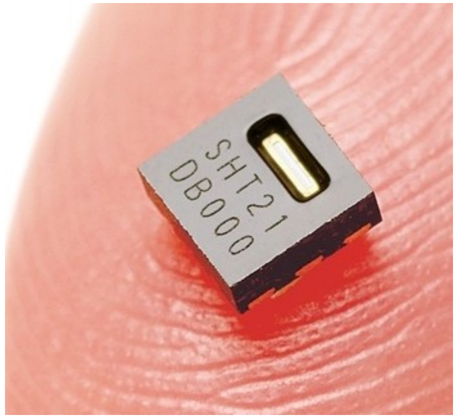

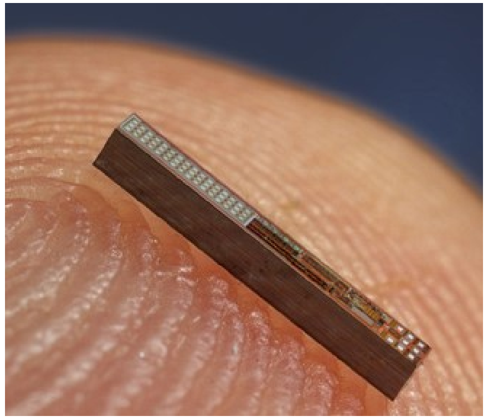

- Internet of Things/Wireless sensor networks
- Active/Semi-active/**Passive RFID**, Wearable/Implantable devices
- Temperature compensation for various sensors

Passive EPC Gen2 RFID Sense Tag Protocol

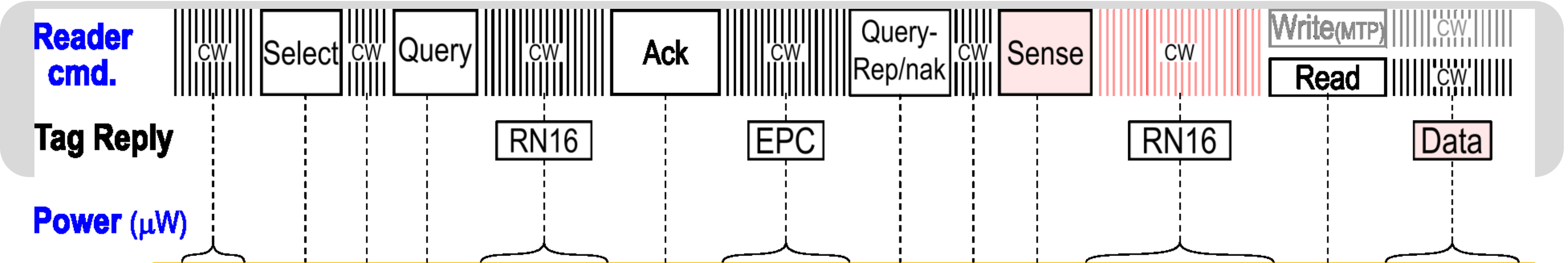

bb	2.4	2.2	3.0	2.3	2.9	2.3	2.6	2.3	2.9	2.3	2.6	2.3	2.9	2.3	2.9	2.3	0.7	2.6	2.3	2.9	2.3	2.6	2.3
demod.	0	1	1	1	1	1	0	1	1	1	0	1	1	1	1	1	0	0	1	1	1	0	1
mod.	0	0	0	0	0	0	0.2	0	0	0	0.2	0	0	0	0	0	0	0.2	0	0	0	0.2	0
clk_bb	0.7	0.7	0.7	0.7	0.7	0.7	0.7	0.7	0.7	0.7	0.7	0.7	0.7	0.7	0.7	0.7	0.7	0.7	0.7	0.7	0.7	0.7	0.7
pmu	3.3	3.3	3.3	3.3	3.3	3.3	3.3	3.3	3.3	3.3	3.3	3.3	3.3	3.3	3.3	3.3	3.3	3.3	3.3	3.3	3.3	3.3	3.3
sen.	0	0	0	0	0	0	0	0	0	0	0	0	0	0	0	0	1.5	0	0	0	0	0	0
clk/dig_s	0	0	0	0	0	0	0	0	0	0	0	0	0	0	0	0	4.0	0	0	0	0	0	0
mtp read	1.4	0	0	0	0	0	0	0	0	0	0	0	0	0	0	0	0	0	0	0	0	0	0
mtp write	0	0	0	0	0	0	0	0	0	0	0	0	0	0	0	0	0	0	0	0	15	0	0
Tag total	7.8	7.2	8.0	7.3	7.9	7.3	6.8	7.3	7.9	7.3	6.8	7.3	7.9	7.3	7.9	7.3	10.2	6.8	7.3	7.9	22.3 7.3	6.8	7.3

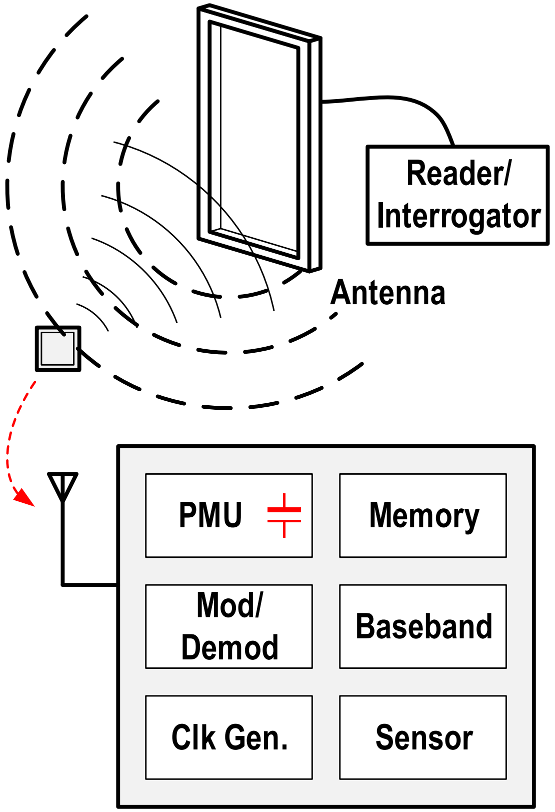

- Operating frequency: 860~960MHz (Half duplex)
- Reader commands: Select (select), tag inventory (Query, Ack, QueryRep/Nak), and tag access (Sense, MTP read)
- Tag replies: RN16, EPC, and the sensor data.

Passive EPC Gen2 RFID Sense Tag Protocol

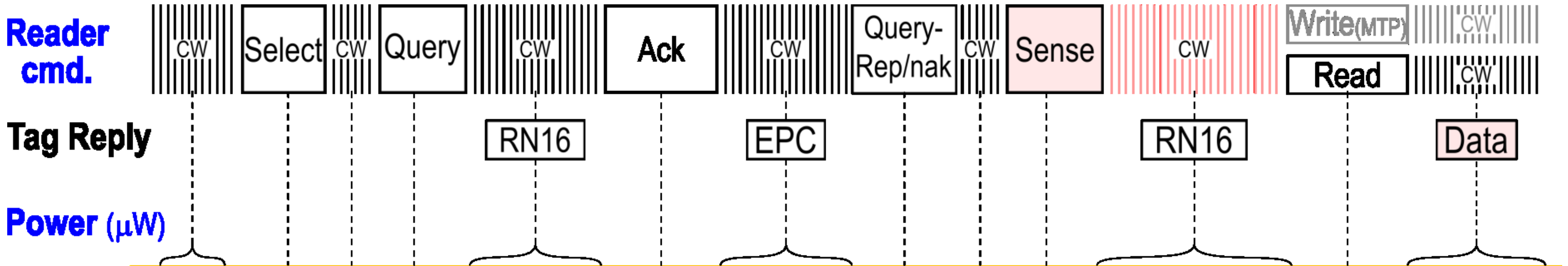

bb	2.4	2.2	3.0	2.3	2.9	2.3	2.6	2.3	2.9	2.3	2.6	2.3	2.9	2.3	2.9	2.3	0.7	2.6	2.3	2.9	2.3	2.6	2.3
demod.	0	1	1	1	1	1	0	1	1	1	0	1	1	1	1	1	0	0	1	1	1	0	1
mod.	0	0	0	0	0	0	0.2	0	0	0	0.2	0	0	0	0	0	0	0.2	0	0	0	0.2	0
clk_bb	0.7	0.7	0.7	0.7	0.7	0.7	0.7	0.7	0.7	0.7	0.7	0.7	0.7	0.7	0.7	0.7	0.7	0.7	0.7	0.7	0.7	0.7	0.7
pmu	3.3	3.3	3.3	3.3	3.3	3.3	3.3	3.3	3.3	3.3	3.3	3.3	3.3	3.3	3.3	3.3	3.3	3.3	3.3	3.3	3.3	3.3	3.3
sen.	0	0	0	0	0	0	0	0	0	0	0	0	0	0	0	0	1.5	0	0	0	0	0	0
clk/dig_s	0	0	0	0	0	0	0	0	0	0	0	0	0	0	0	0	4.0	0	0	0	0	0	0
mtp read	1.4	0	0	0	0	0	0	0	0	0	0	0	0	0	0	0	0	0	0	0	0	0	0
mtp write	0	0	0	0	0	0	0	0	0	0	0	0	0	0	0	0	0	0	0	0	15	0	0
Tag total	7.8	7.2	8.0	7.3	7.9	7.3	6.8	7.3	7.9	7.3	6.8	7.3	7.9	7.3	7.9	7.3	10.2	6.8	7.3	7.9	22.3 / 7.3	6.8	7.3

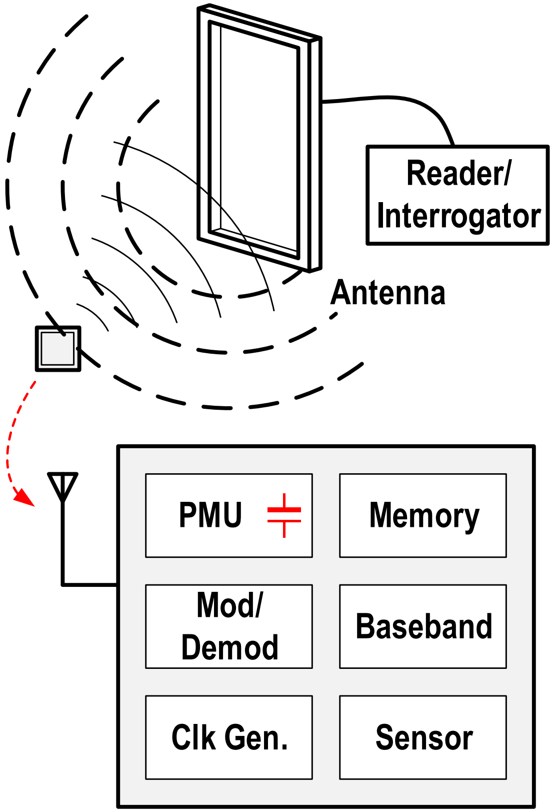

- Tag available power in the order of μW
  - Power down/gating for non-critical circuits
  - Sensor power directly affects the tag sensitivity/reading range
  - e.g. Monza R6 tag with -22 dBm read sensitivity → 2μW sensing power can reduce reading distance by ~2x

Passive EPC Gen2 RFID Sense Tag Protocol

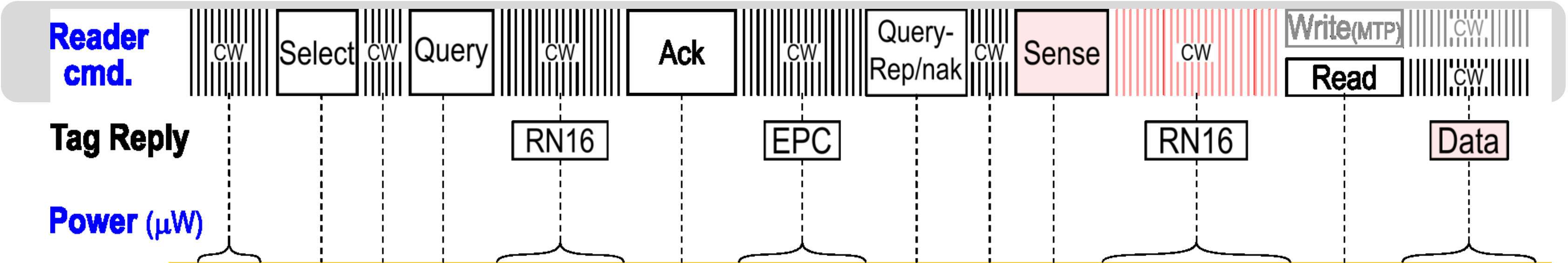

bb	2.4	2.2	3.0	2.3	2.9	2.3	2.6	2.3	2.9	2.3	2.6	2.3	2.9	2.3	2.9	2.3	0.7	2.6	2.3	2.9	2.3	2.6	2.3
demod.	0	1	1	1	1	1	0	1	1	1	0	1	1	1	1	1	0	0	1	1	1	0	1
mod.	0	0	0	0	0	0	0.2	0	0	0	0.2	0	0	0	0	0	0	0.2	0	0	0	0.2	0
clk_bb	0.7	0.7	0.7	0.7	0.7	0.7	0.7	0.7	0.7	0.7	0.7	0.7	0.7	0.7	0.7	0.7	0.7	0.7	0.7	0.7	0.7	0.7	0.7
pmu	3.3	3.3	3.3	3.3	3.3	3.3	3.3	3.3	3.3	3.3	3.3	3.3	3.3	3.3	3.3	3.3	3.3	3.3	3.3	3.3	3.3	3.3	3.3
sen.	0	0	0	0	0	0	0	0	0	0	0	0	0	0	0	0	1.5	0	0	0	0	0	0
clk/dig_s	0	0	0	0	0	0	0	0	0	0	0	0	0	0	0	0	4.0	0	0	0	0	0	0
mtp read	1.4	0	0	0	0	0	0	0	0	0	0	0	0	0	0	0	0	0	0	0	0	0	0
mtp write	0	0	0	0	0	0	0	0	0	0	0	0	0	0	0	0	0	0	0	0	15	0	0
Tag total	7.8	7.2	8.0	7.3	7.9	7.3	6.8	7.3	7.9	7.3	6.8	7.3	7.9	7.3	7.9	7.3	10.2	6.8	7.3	7.9	22.3 / 7.3	6.8	7.3

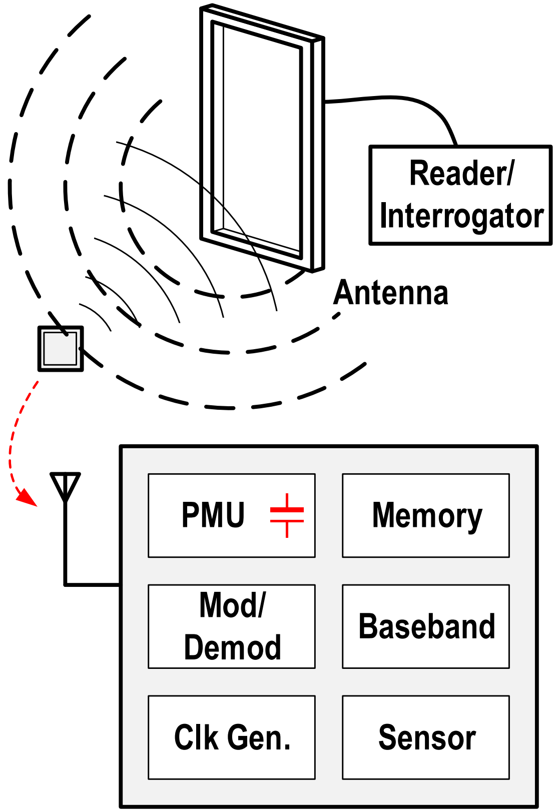

- Passively-powered with limited on-chip supply filtering
  - High Power Efficiency vs. High Energy Efficiency
  - Burst mode operation can be tricky (e.g. a 50ns/8mA current spike → 0.4V drop w/ 1nF on chip capacitor)
  - Sensor w/ good supply immunity (speed vs. precision)

Passive EPC Gen2 RFID Sense Tag Protocol

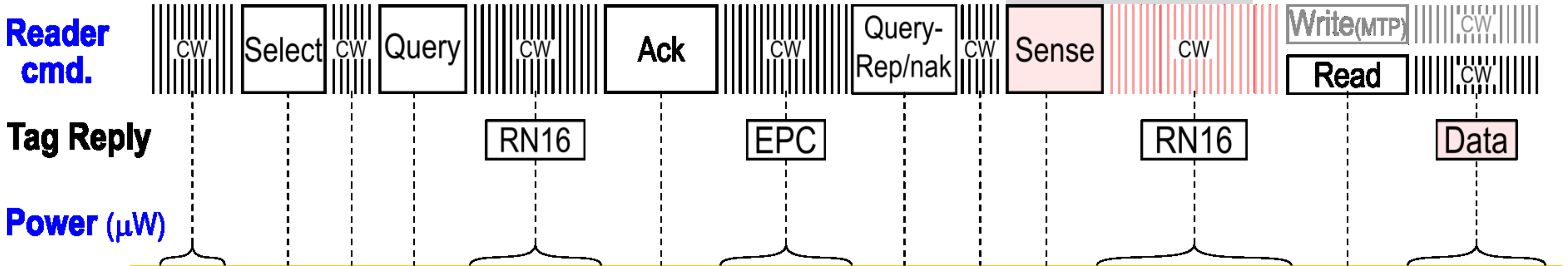

bb	2.4	2.2	3.0	2.3	2.9	2.3	2.6	2.3	2.9	2.3	2.6	2.3	2.9	2.3	2.9	2.3	0.7	2.6	2.3	2.9	2.3	2.6	2.3
demod.	0	1	1	1	1	1	0	1	1	1	0	1	1	1	1	1	0	0	1	1	1	0	1
mod.	0	0	0	0	0	0	0.2	0	0	0	0.2	0	0	0	0	0	0	0.2	0	0	0	0.2	0
clk_bb	0.7	0.7	0.7	0.7	0.7	0.7	0.7	0.7	0.7	0.7	0.7	0.7	0.7	0.7	0.7	0.7	0.7	0.7	0.7	0.7	0.7	0.7	0.7
pmu	3.3	3.3	3.3	3.3	3.3	3.3	3.3	3.3	3.3	3.3	3.3	3.3	3.3	3.3	3.3	3.3	3.3	3.3	3.3	3.3	3.3	3.3	3.3
sen.	0	0	0	0	0	0	0	0	0	0	0	0	0	0	0	0	1.5	0	0	0	0	0	0
clk/dig_s	0	0	0	0	0	0	0	0	0	0	0	0	0	0	0	0	4.0	0	0	0	0	0	0
mtp read	1.4	0	0	0	0	0	0	0	0	0	0	0	0	0	0	0	0	0	0	0	0	0	0
mtp write	0	0	0	0	0	0	0	0	0	0	0	0	0	0	0	0	0	0	0	0	15	0	0
Tag total	7.8	7.2	8.0	7.3	7.9	7.3	6.8	7.3	7.9	7.3	6.8	7.3	7.9	7.3	7.9	7.3	10.2	6.8	7.3	7.9	22.3 7.3	6.8	7.3

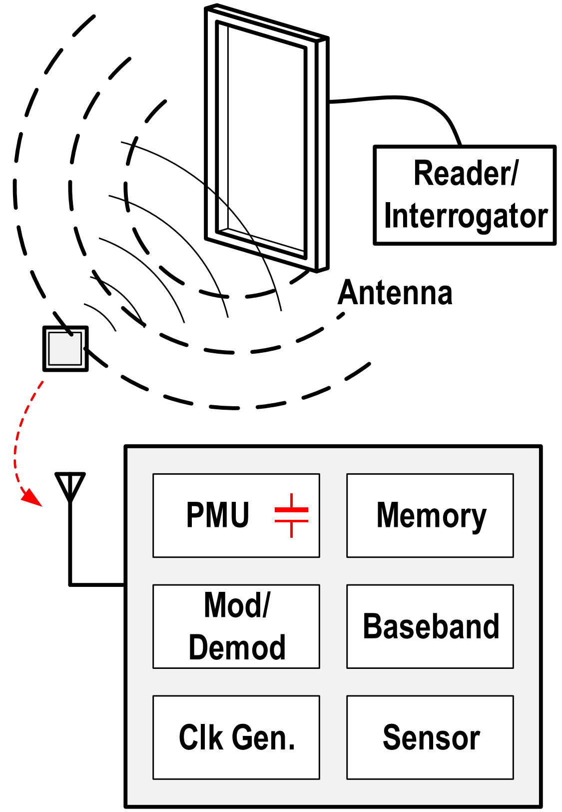

- EPC protocol compliant
  - Convert regular commands into custom sensing command for protocol compliance
  - Sensing time limited by the link timing at 20ms maximum
  - Immediate reply, delayed reply, in-process reply

Passive EPC Gen2 RFID Sense Tag Protocol

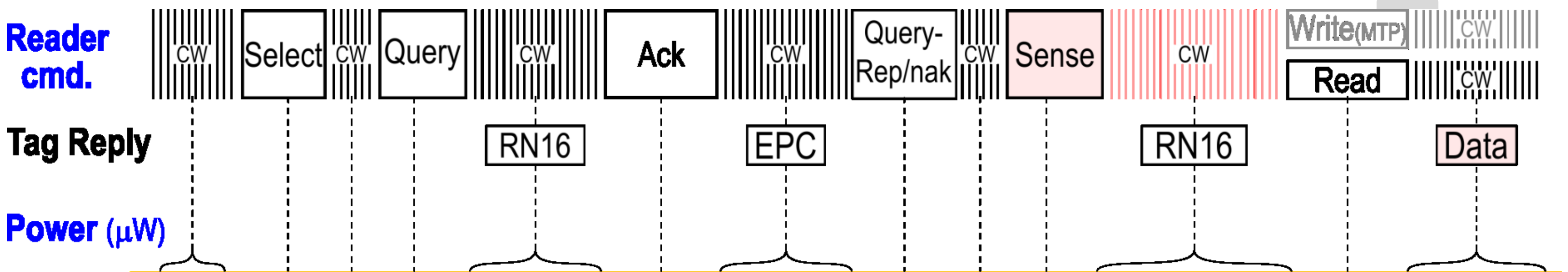

bb	2.4	2.2	3.0	2.3	2.9	2.3	2.6	2.3	2.9	2.3	2.6	2.3	2.9	2.3	2.9	2.3	0.7	2.6	2.3	2.9	2.3	2.6	2.3
demod.	0	1	1	1	1	1	0	1	1	1	0	1	1	1	1	1	0	0	1	1	1	0	1
mod.	0	0	0	0	0	0	0.2	0	0	0	0.2	0	0	0	0	0	0	0.2	0	0	0	0.2	0
clk_bb	0.7	0.7	0.7	0.7	0.7	0.7	0.7	0.7	0.7	0.7	0.7	0.7	0.7	0.7	0.7	0.7	0.7	0.7	0.7	0.7	0.7	0.7	0.7
pmu	3.3	3.3	3.3	3.3	3.3	3.3	3.3	3.3	3.3	3.3	3.3	3.3	3.3	3.3	3.3	3.3	3.3	3.3	3.3	3.3	3.3	3.3	3.3
sen.	0	0	0	0	0	0	0	0	0	0	0	0	0	0	0	0	1.5	0	0	0	0	0	0
clk/dig_s	0	0	0	0	0	0	0	0	0	0	0	0	0	0	0	0	4.0	0	0	0	0	0	0
mtp read	1.4	0	0	0	0	0	0	0	0	0	0	0	0	0	0	0	0	0	0	0	0	0	0
mtp write	0	0	0	0	0	0	0	0	0	0	0	0	0	0	0	0	0	0	0	0	15	0	0
Tag total	7.8	7.2	8.0	7.3	7.9	7.3	6.8	7.3	7.9	7.3	6.8	7.3	7.9	7.3	7.9	7.3	10.2	6.8	7.3	7.9	22.3 / 7.3	6.8	7.3

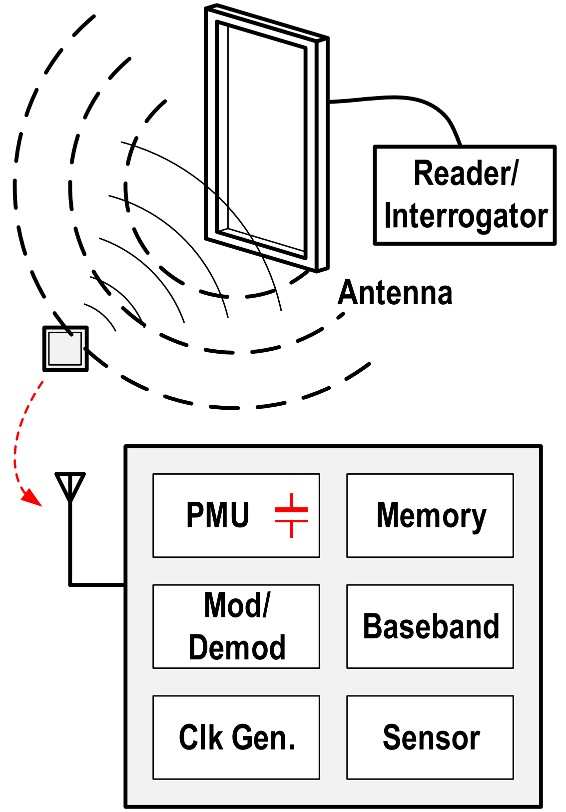

- MTP writing consumes most power
  - Avoid MTP writing for sensing
  - Store sensor data with customized data storage with long retention time (tens to hundreds of ms)

Passive EPC Gen2 RFID Sense Tag Protocol

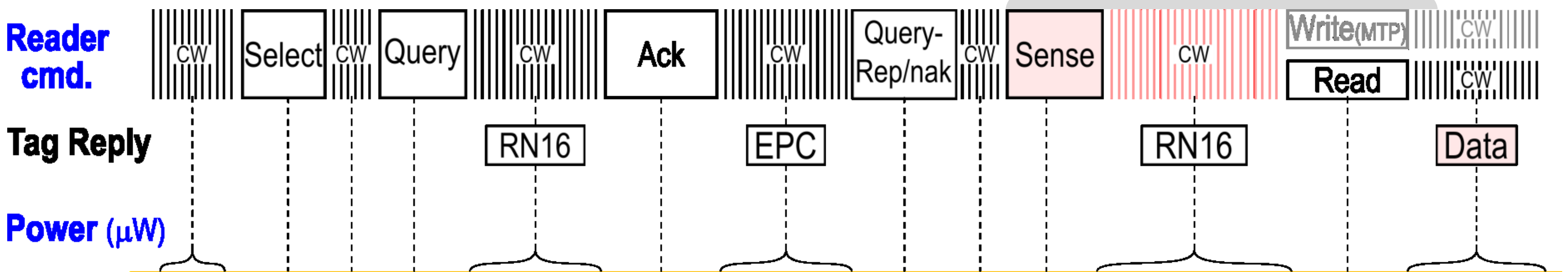

bb	2.4	2.2	3.0	2.3	2.9	2.3	2.6	2.3	2.9	2.3	2.6	2.3	2.9	2.3	2.9	2.3	0.7	2.6	2.3	2.9	2.3	2.6	2.3
demod.	0	1	1	1	1	1	0	1	1	1	0	1	1	1	1	1	0	0	1	1	1	0	1
mod.	0	0	0	0	0	0	0.2	0	0	0	0.2	0	0	0	0	0	0	0.2	0	0	0	0.2	0
clk_bb	0.7	0.7	0.7	0.7	0.7	0.7	0.7	0.7	0.7	0.7	0.7	0.7	0.7	0.7	0.7	0.7	0.7	0.7	0.7	0.7	0.7	0.7	0.7
pmu	3.3	3.3	3.3	3.3	3.3	3.3	3.3	3.3	3.3	3.3	3.3	3.3	3.3	3.3	3.3	3.3	3.3	3.3	3.3	3.3	3.3	3.3	3.3
sen.	0	0	0	0	0	0	0	0	0	0	0	0	0	0	0	0	1.5	0	0	0	0	0	0
clk/dig_s	0	0	0	0	0	0	0	0	0	0	0	0	0	0	0	0	4.0	0	0	0	0	0	0
mtp read	1.4	0	0	0	0	0	0	0	0	0	0	0	0	0	0	0	0	0	0	0	0	0	0
mtp write	0	0	0	0	0	0	0	0	0	0	0	0	0	0	0	0	0	0	0	0	15	0	0
Tag total	7.8	7.2	8.0	7.3	7.9	7.3	6.8	7.3	7.9	7.3	6.8	7.3	7.9	7.3	7.9	7.3	10.2	6.8	7.3	7.9	22.3 7.3	6.8	7.3

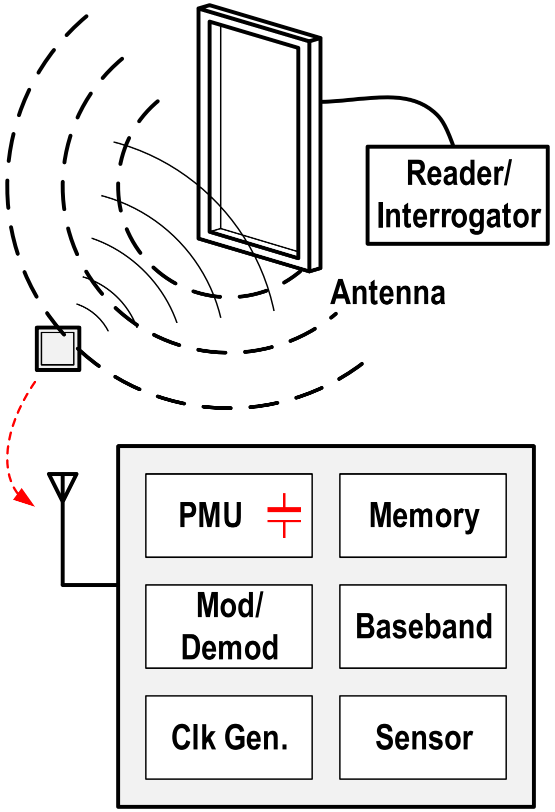

- Sensor Calibration
  - One-point calibration is necessary for maintenance and deployment cost reduction
  - Wireless operation to relax the calibration cost/effort
  - Multiple sensor calibration possible

CMOS Temperature Sensors

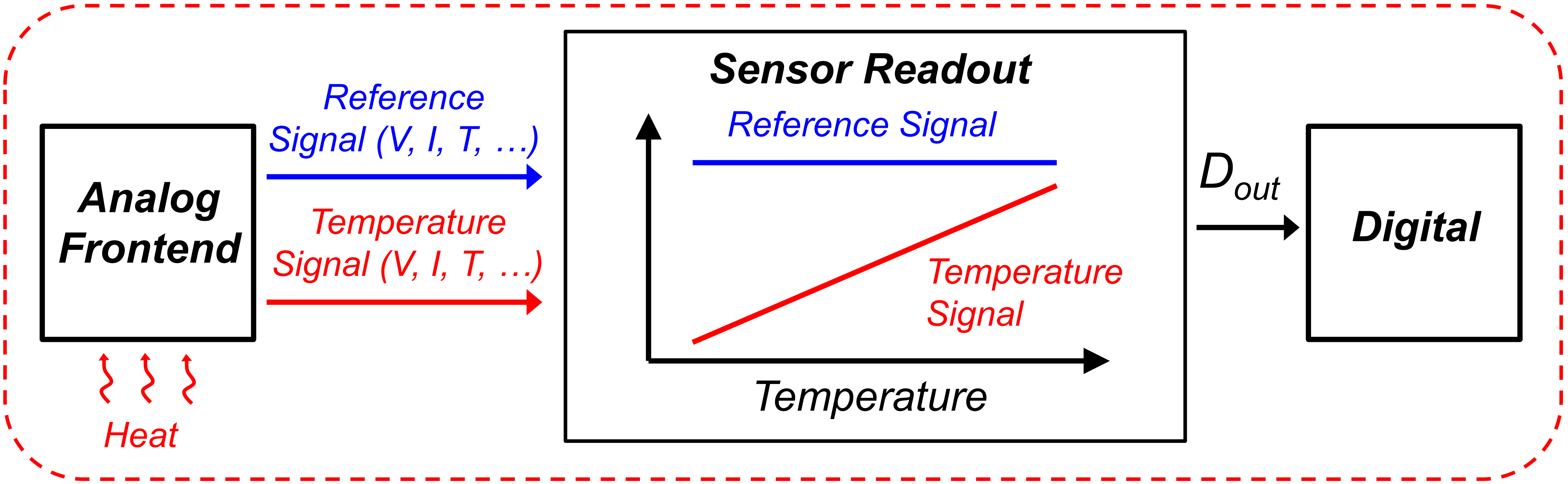

- Analog frontend
  - BJTs, MOSFETs, on-chip resistors etc.
- Sensor readout
  - Analog-to-digital converter (e.g. I-ADC, SAR), Time-to-digital/Frequency-to-digital converters (TDC/FDC)

CMOS Temperature Sensors Survey

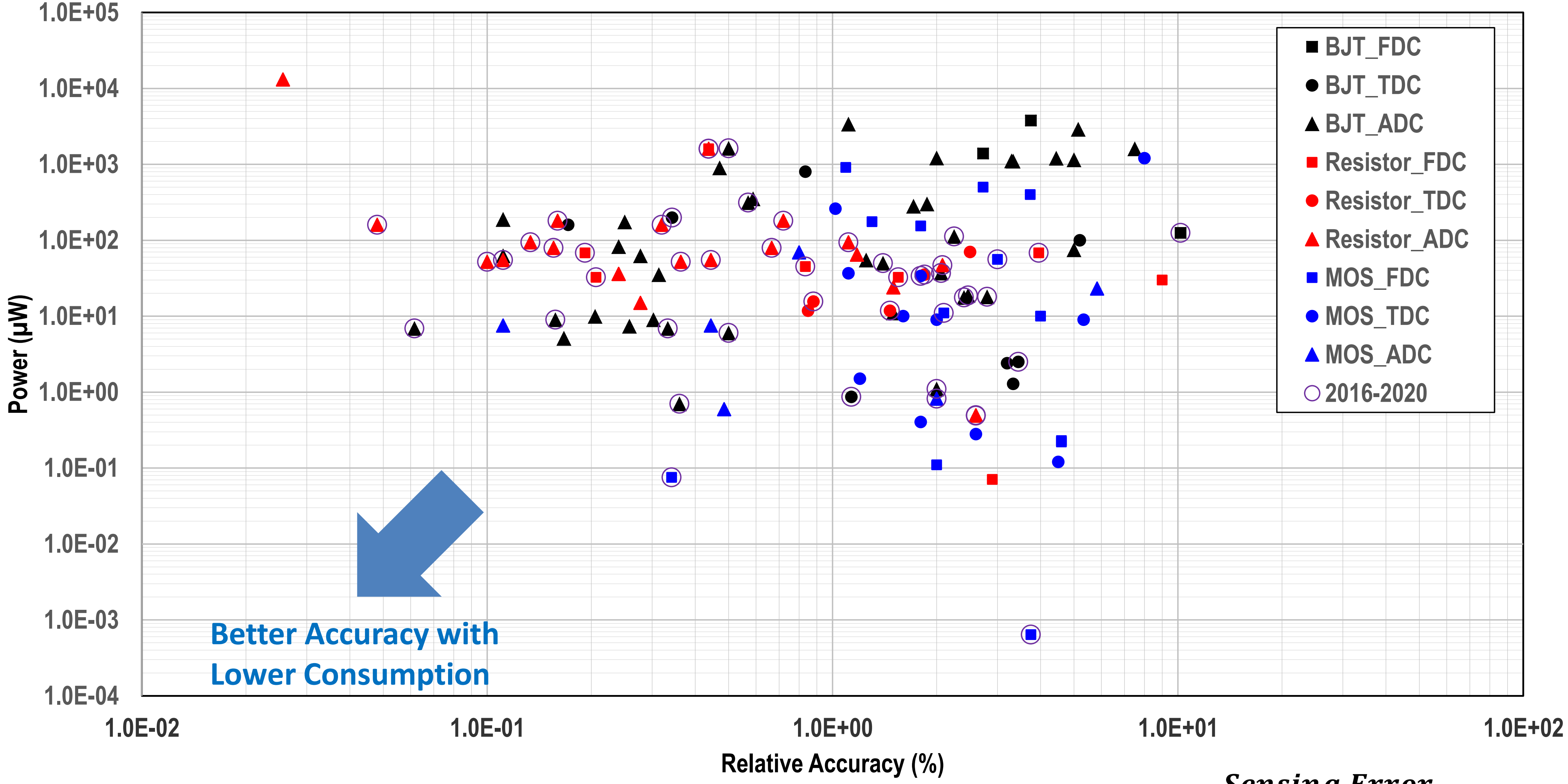

[K. Makinwa, Smart Temperature Sensor Performance Survey]

$$Rel.\,Acc. = \frac{Sensing\ Error}{Sensing\ Range} \cdot 100\%$$

CMOS Temperature Sensors Survey

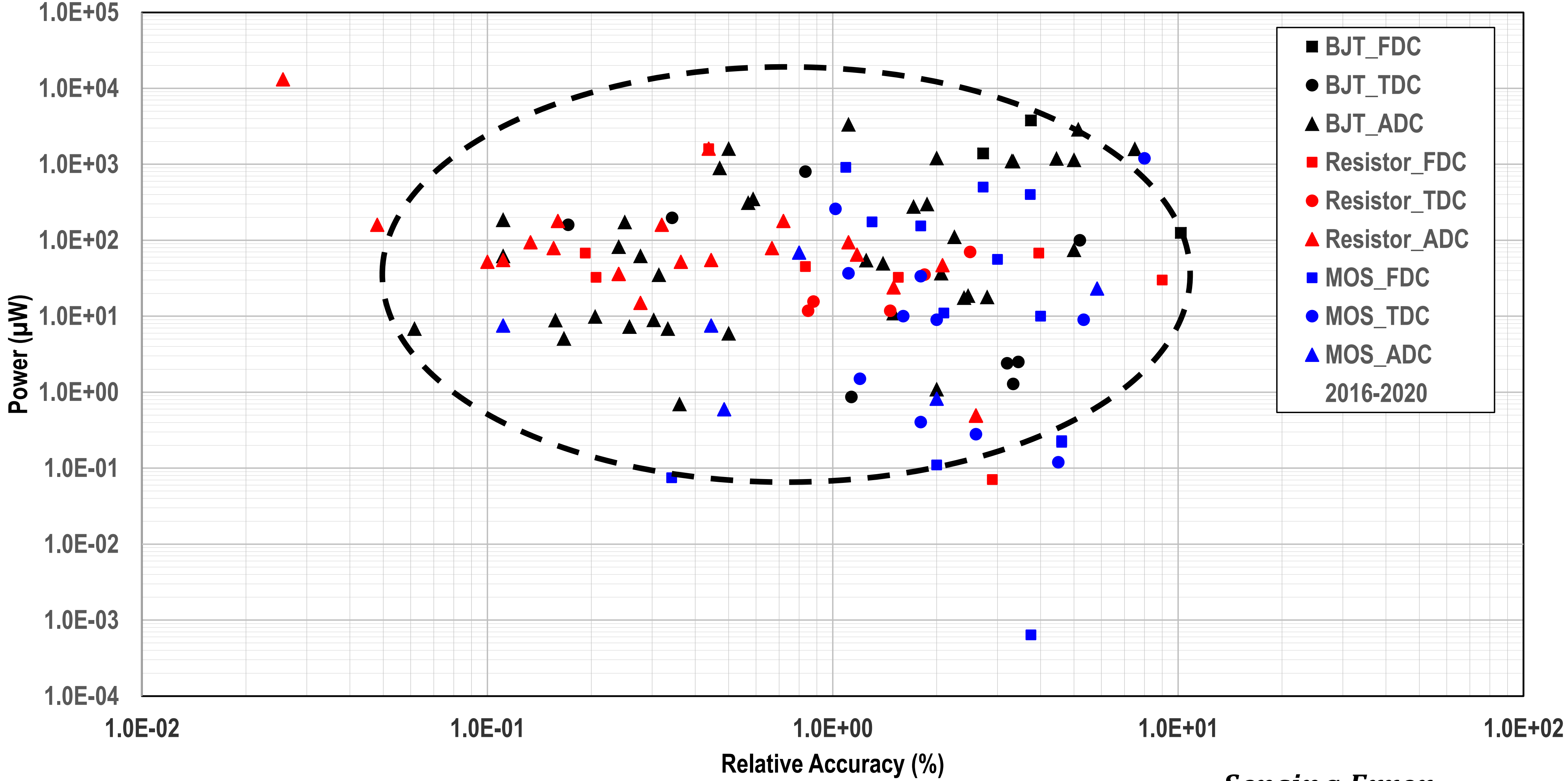

[K. Makinwa, Smart Temperature Sensor Performance Survey]

$$Rel.Acc. = \frac{Sensing\ Error}{Sensing\ Range} \cdot 100\%$$

CMOS Temperature Sensors Survey

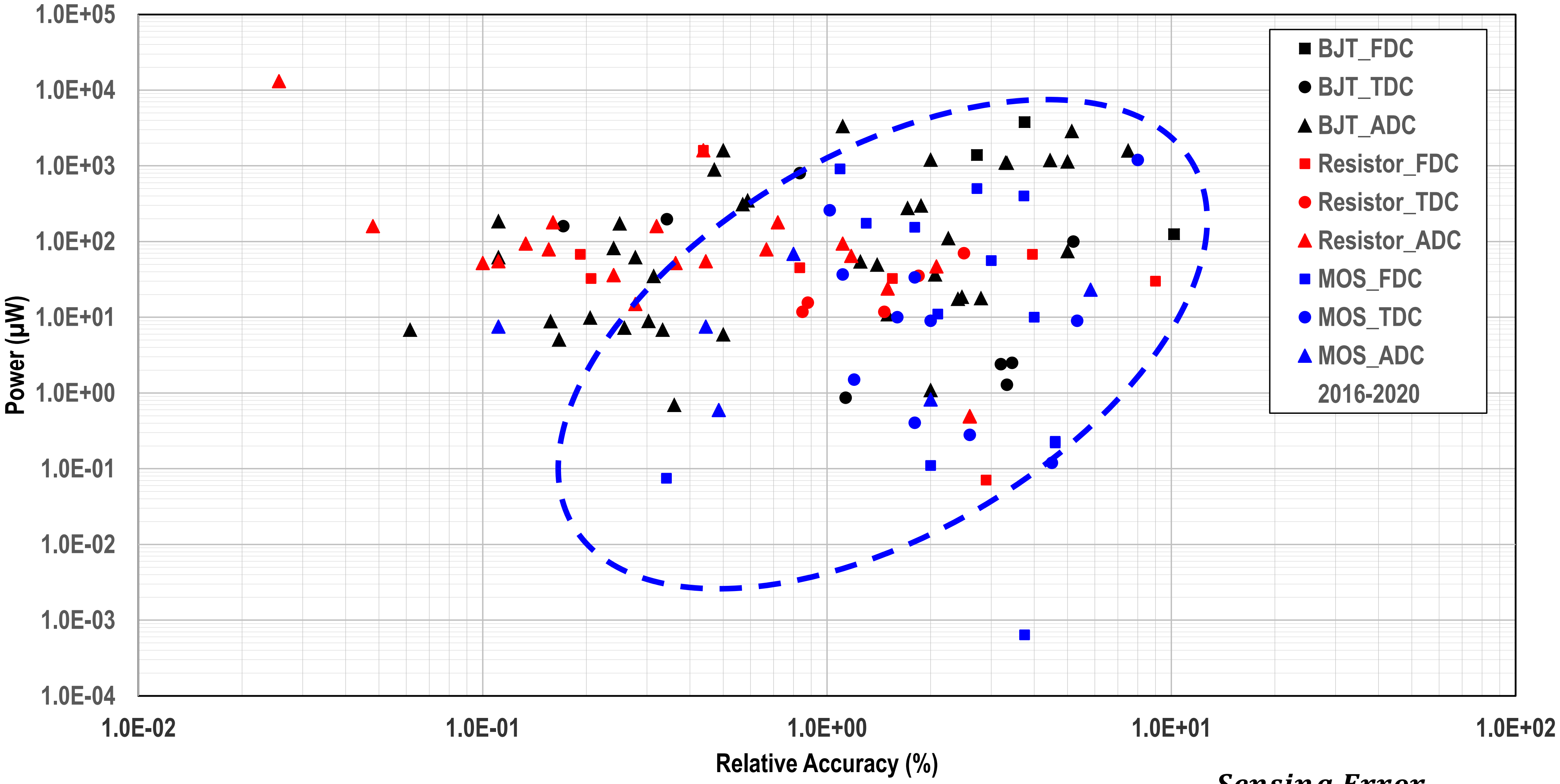

[K. Makinwa, Smart Temperature Sensor Performance Survey]

$$Rel.\,Acc. = \frac{Sensing\ Error}{Sensing\ Range} \cdot 100\%$$

CMOS Temperature Sensors Survey

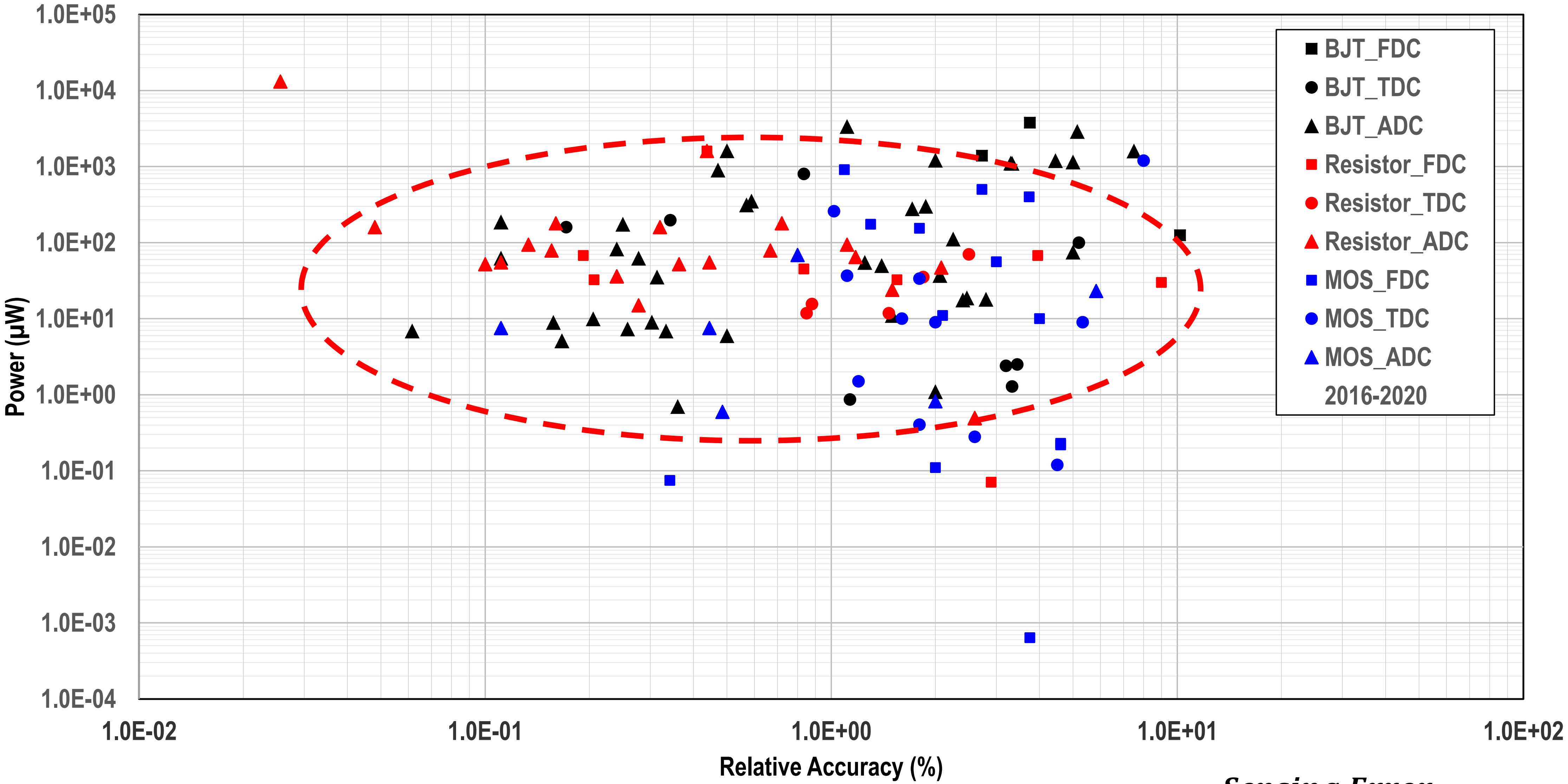

[K. Makinwa, Smart Temperature Sensor Performance Survey]

$$Rel.Acc. = \frac{Sensing\ Error}{Sensing\ Range} \cdot 100\%$$

CMOS Temperature Sensors Survey

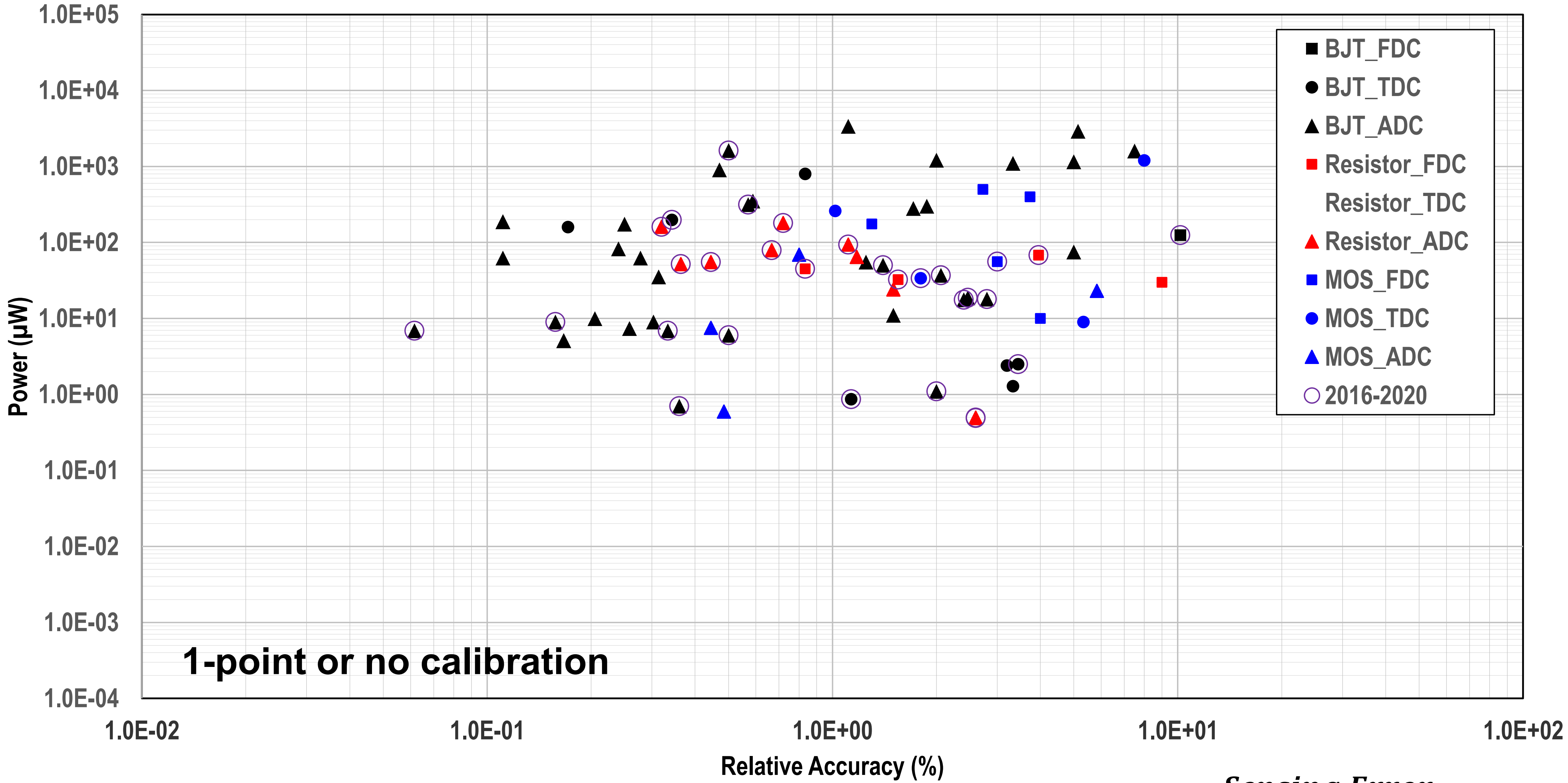

[K. Makinwa, Smart Temperature Sensor Performance Survey]

$$Rel.Acc. = \frac{Sensing\ Error}{Sensing\ Range} \cdot 100\%$$

CMOS Temperature Sensors Survey

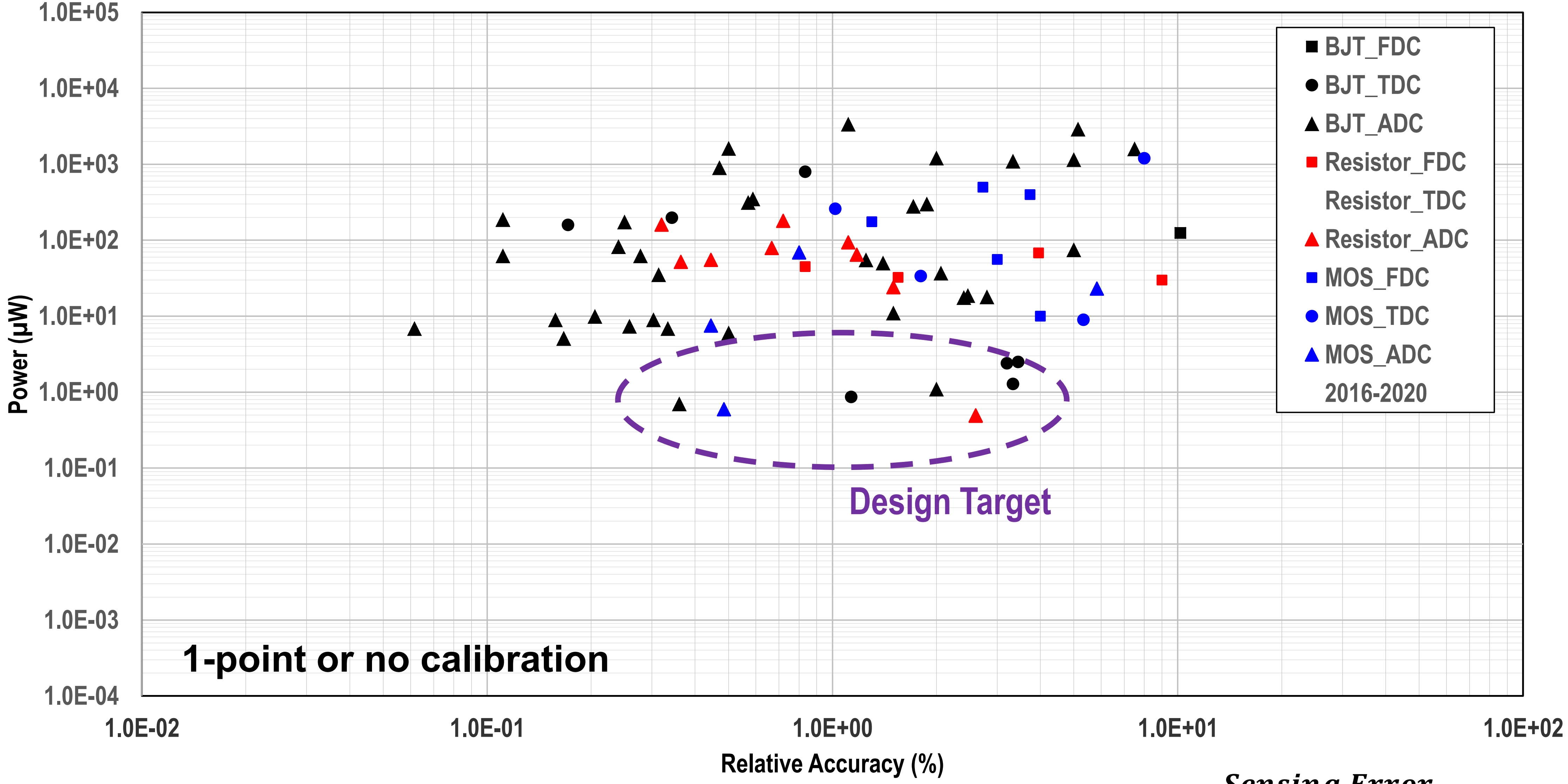

[K. Makinwa, Smart Temperature Sensor Performance Survey]

$$Rel.Acc. = \frac{Sensing\ Error}{Sensing\ Range} \cdot 100\%$$

CMOS Temperature Sensors Survey

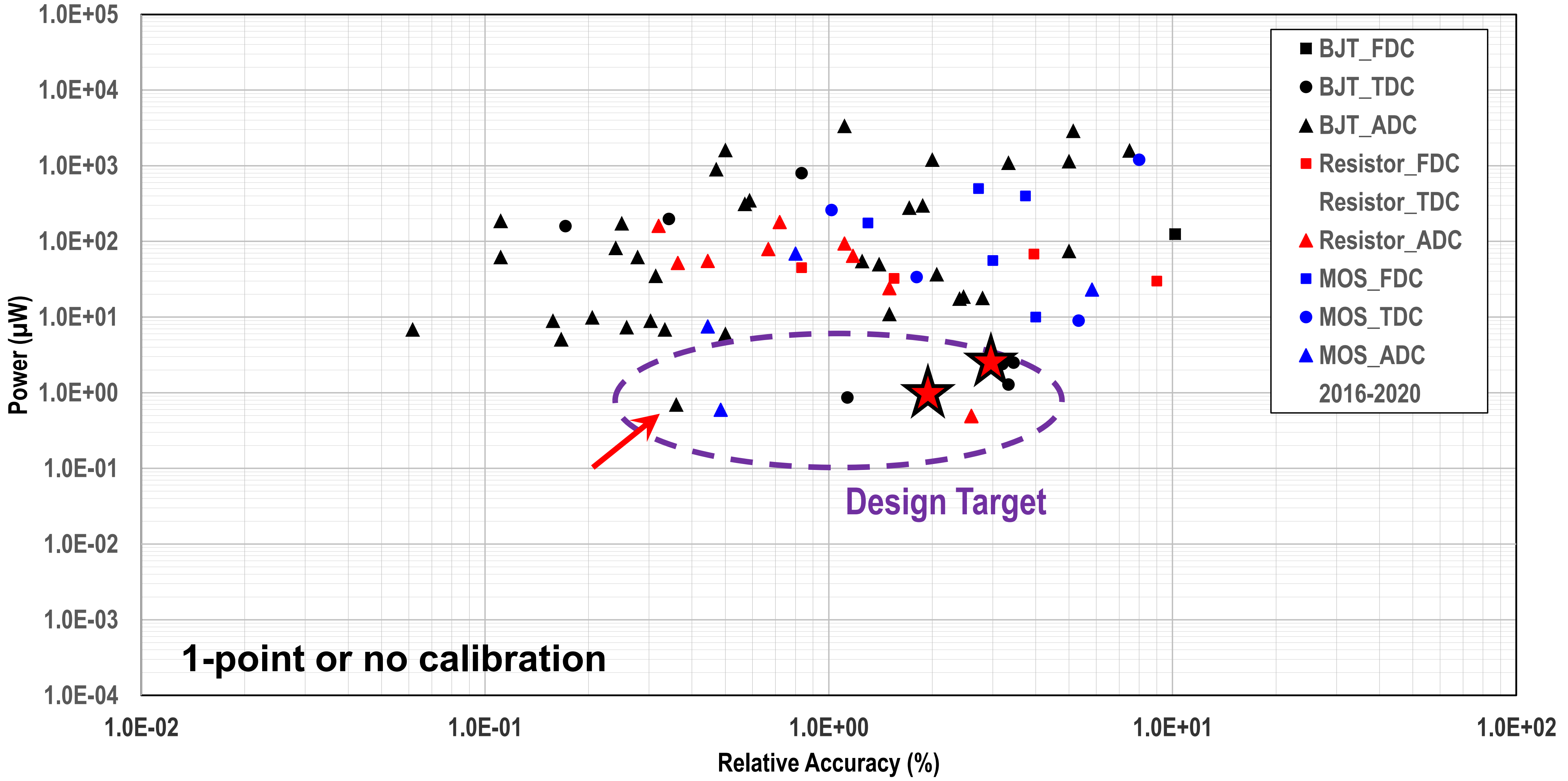

[K. Makinwa, Smart Temperature Sensor Performance Survey]

Outline

- Motivation and Challenge
- Fundamentals of BJT-based CMOS Temperature Sensing
- Design Examples
  - Ultra-low Power High Accuracy CMOS Temperature Sensor for Clinical Temperature Monitoring
  - Embedded Time-Domain Wide Sensing Range CMOS Temperature Sensor
- Conclusions

BJT for Temperature Sensing

- Vertical/Lateral PNP/NPN BJT
- For a BJT, the collector current I_C is dependent on the base-emitter voltage V_{BE}

$$I_C = I_S \cdot \left(e^{\frac{V_{BE}}{kT/q}} - 1\right) \approx I_S \cdot e^{\frac{V_{BE}}{kT/q}}$$

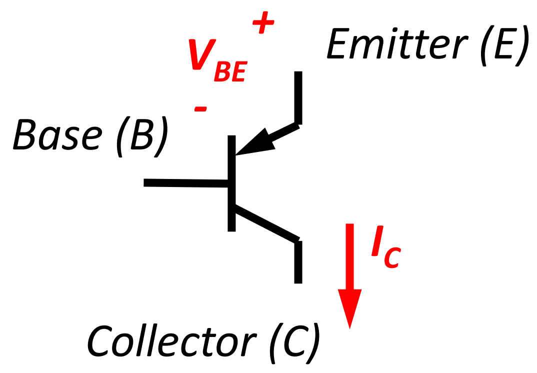

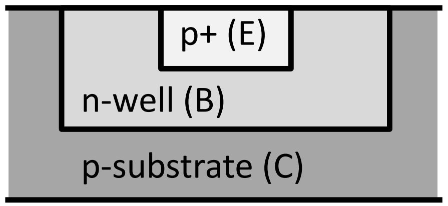

- The saturation current I_S exhibits strong temperature dependence

$$I_S = A_E \cdot C \cdot T^{\eta} \cdot e^{-\frac{V_{g0}}{kT/q}}$$

- A_E = emitter area, C is a process dependent term, $\eta \approx$ 3~4, V_{g0} is the extrapolated bandgap voltage of silicon

V_{BE} and ΔV_{BE} Characteristics

- For $I_C >> I_S$

$$V_{BE} = \frac{kT}{q} ln \frac{I_C}{I_S}$$

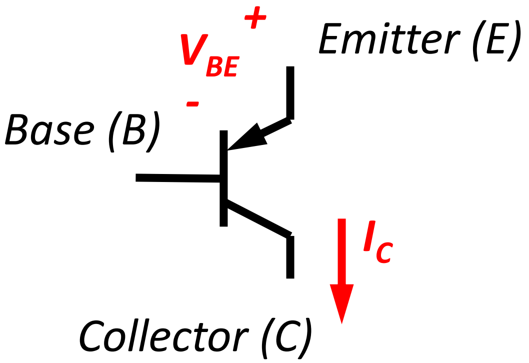

- V_{BE} is complementary-to-absolute-temperature (CTAT) and non-linear, as governed by I_S, and is therefore process dependent

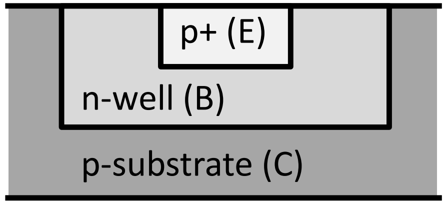

- The I_S term can be eliminated by measuring the difference of two collector currents

$$\Delta V_{BE} = V_{BE2} - V_{BE1} = \frac{kT}{q} ln \frac{I_{C2}}{I_{C1}}$$

V_{BE} and ΔV_{BE} Characteristics

- By controlling the collector current ratio (*p*) and emitter-area ratio (*r*)

$$\Delta V_{BE} = V_{BE2} - V_{BE1} = \frac{kT}{q} ln(k \cdot r)$$

- With *p* = 5 and *r* = 1, ΔV_{BE} ~ 126 µV/°C

- ΔV_{BE} is process tolerant with highly linearity and proportional-to-absolute-temperature (PTAT)

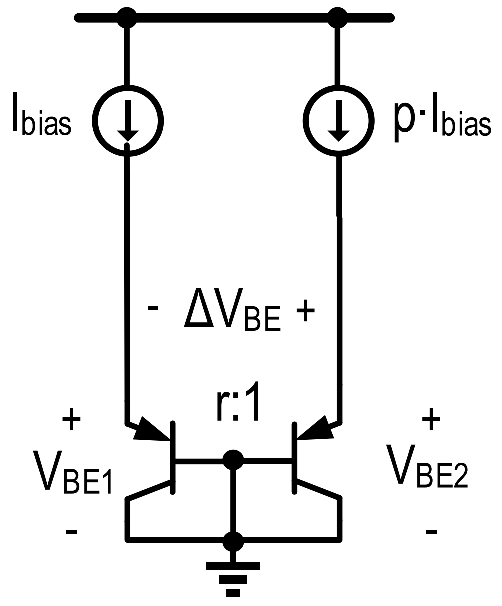

Basic Operation Principle

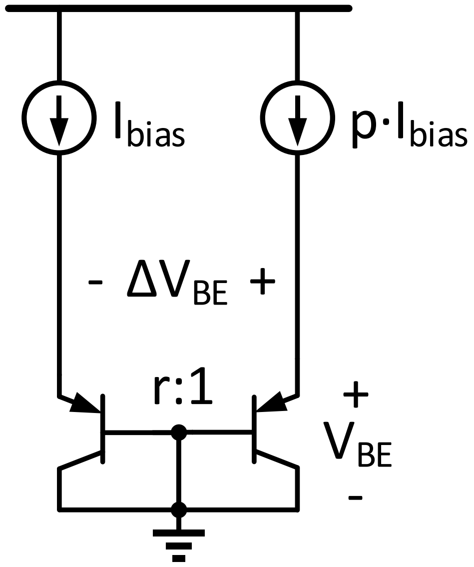

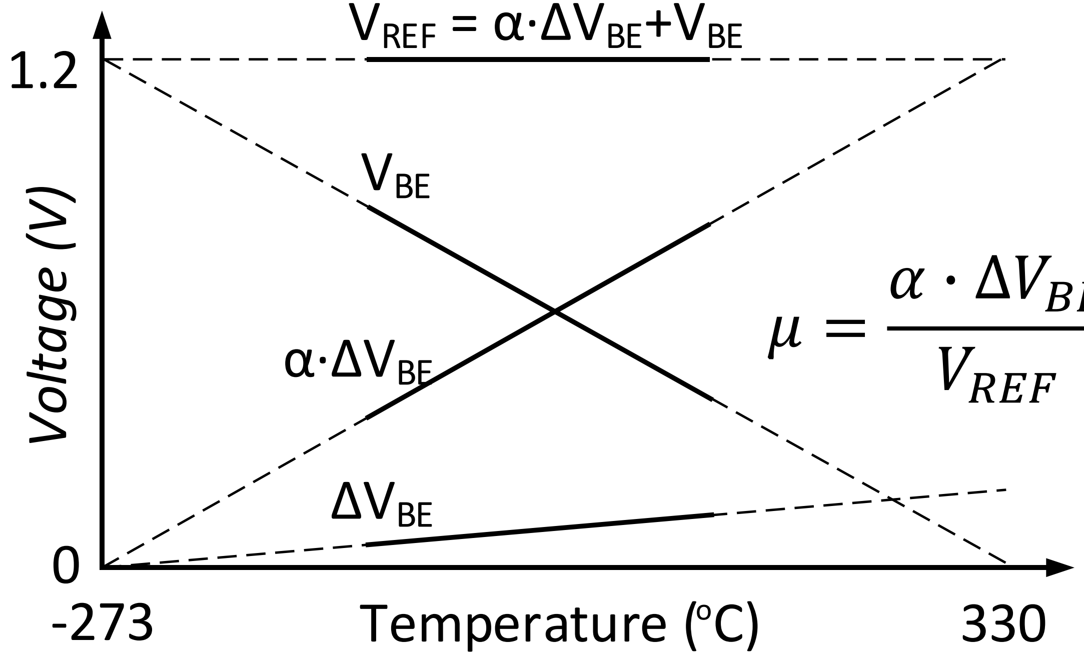

$$\mu = \frac{\alpha \cdot \Delta V_{BE}}{V_{REF}}$$

- Two BJTs biased at different current densities for generating
  - ΔV_{BE} : Proportional-to-absolute-temperature (PTAT)
  - V_{BE} : Complementary-to-absolute-temperature (CTAT)
- V_{REF} generated by linear combination of αV_{BE} and ΔV_{BE} (α is the prop. constant)
- Signal FS from -273 to 300°C → 16-bit for 0.01°C resolution

Non-linearity in V_{BE}

- For practical reasons, I_C is generally made proportional to some power of T, with m typically = -1, 0, 1

$$I_C \propto T^m = I_C(T_r)\left(\frac{T}{T_r}\right)^m \qquad I_C = A_E C T^{\eta} e^{\frac{V_{BE}-V_{g0}}{kT/q}}$$

- Express V_{BE} as the sum of a constant term, a proportional to T term, and higher-order terms

$$V_{BE} = \underbrace{V_{BE0}} - \underbrace{\lambda T} + \underbrace{c(T)}$$

$$\boxed{V_{BE0} = V_{g0} + (\eta - m)\frac{kT_r}{q}} \quad \boxed{\lambda = \frac{V_{BE0} - V_{BE}(T_r)}{T_r}} \quad \boxed{c(T) = (\eta - m)\frac{k}{q}\left(T - T_r - T \cdot ln\frac{T}{T_r}\right)}$$

Non-linearity in V_{BE}

$$V_{BE0} = V_{g0} + (\eta - m)\frac{kT_r}{q}$$

$$\boxed{V_{BE} = V_{BE0} - \lambda T + c(T)}$$

$$\lambda = \frac{V_{BE0} - V_{BE}(T_r)}{T_r} \rightarrow -2mV/^oC$$

$$c(T) = (\eta - m)\frac{k}{q}\left(T - T_r - T \cdot ln\frac{T}{T_r}\right) < 0$$

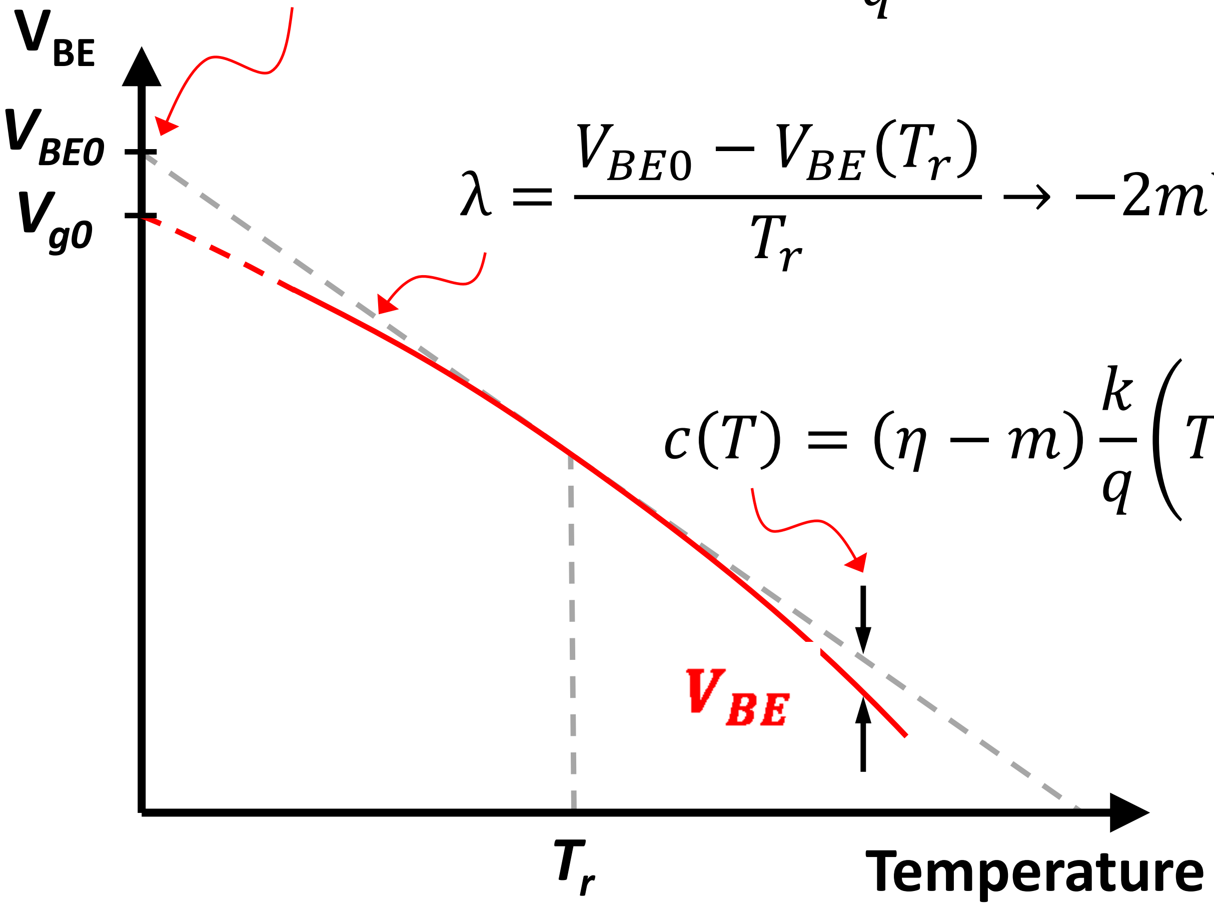

$V_{g0} \approx 1.156V$ @ T_r=300K

- V_{BE} is CTAT
- V_{BE} is a convex function of temperature

I_S Process Spread

- Process mainly impacts I_S
  - Base doping
  - Geometry

- Process spread in I_S
  $\rightarrow$ process spread in V_{BE}

$$\delta V_{BE} \propto -\frac{kT}{q} \cdot \frac{\delta I_S}{I_S}$$

- V_{BE} spread is PTAT
  $\rightarrow$ can be PTAT trimmed (e.g. by adjusting I_C)

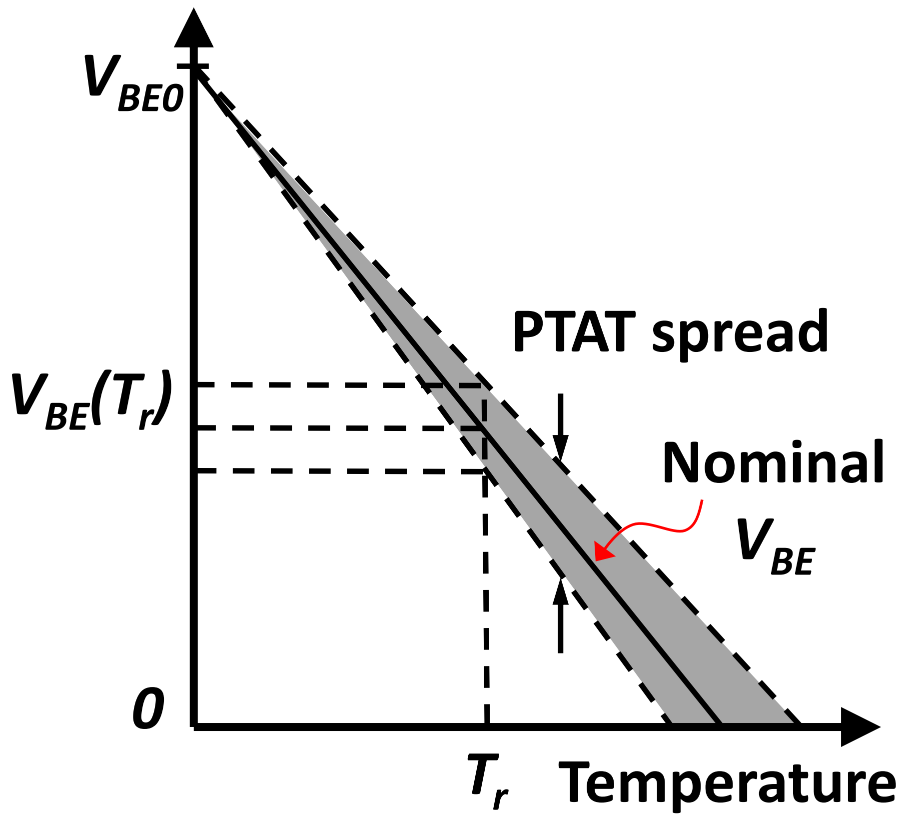

Current gain in BJT

- I_{bias} is I_E instead of I_C
- With current gain β_F

$$V_{BE} = \frac{kT}{q} ln\left(\frac{I_{bias}}{I_S} \cdot \frac{\beta_F}{\beta_F + 1}\right)$$

$$\Delta V_{BE} = \frac{kT}{q} ln\left(\frac{I_{C2}}{I_{C1}}\right) = \frac{kT}{q} ln\left(\frac{\beta_{F1}}{\beta_{F2}} \cdot \frac{\beta_{F2} + 1}{\beta_{F1} + 1} \cdot \frac{I_{E2}}{I_{E1}}\right)$$

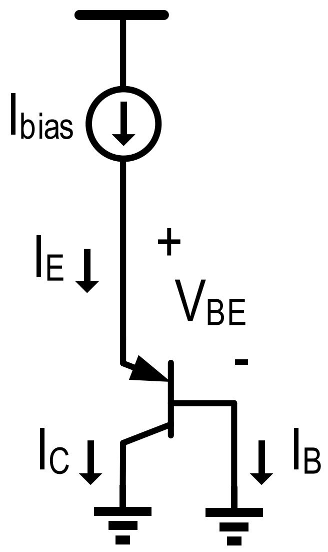

- Current gain variation induces non-PTAT spread

$$\delta V_{BE} = \frac{kT}{q}\frac{\delta\alpha_F}{\alpha_F} = \frac{kT}{q}\frac{1}{1+\beta_F} \cdot \frac{\delta\beta_F}{\beta_F}$$

$$I_C = \alpha_F I_E = \frac{\beta_F I_E}{\beta_F + 1}$$

$$\beta_F = \beta_{F0}\left(\frac{T}{T_r}\right)^{XTB}$$

Biasing for BJT

- Assuming $I_C >> I_S$

$$I_C = I_S\left(e^{\frac{V_{BE}}{kT/q}} - 1\right)$$

$$\Delta V_{BE} = \frac{kT}{q} ln\left(\frac{nI_{C1} + I_S}{I_{C1} + I_S}\right)$$

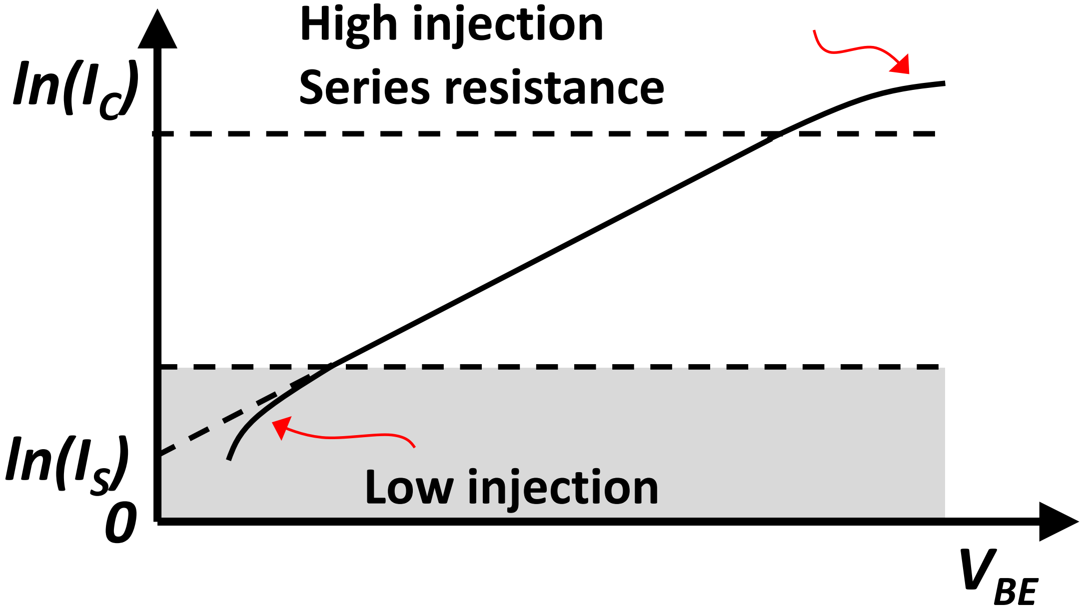

- Constant β_F biasing

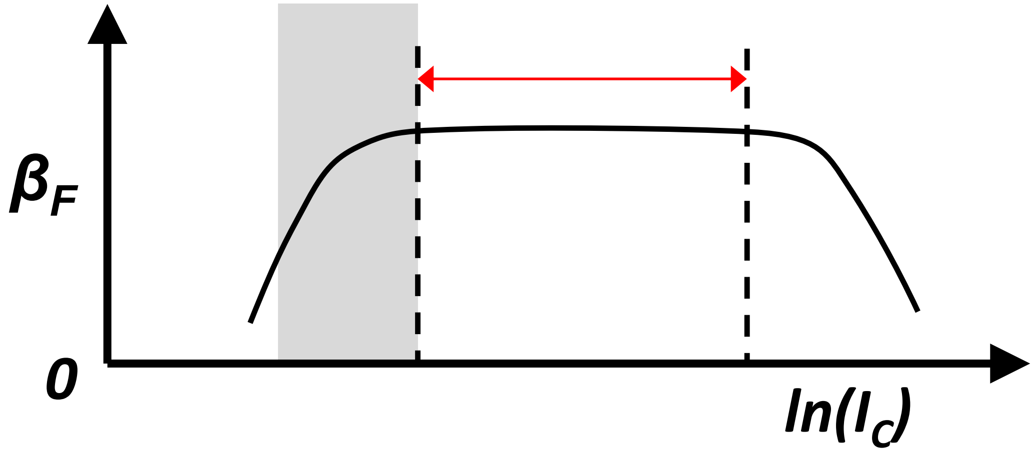

System Error Sources

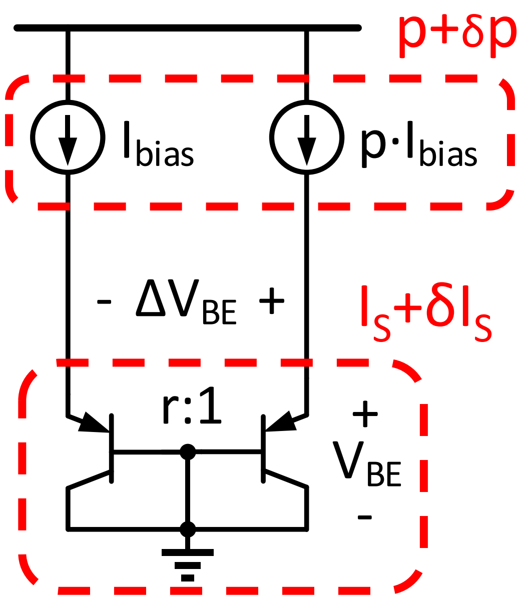

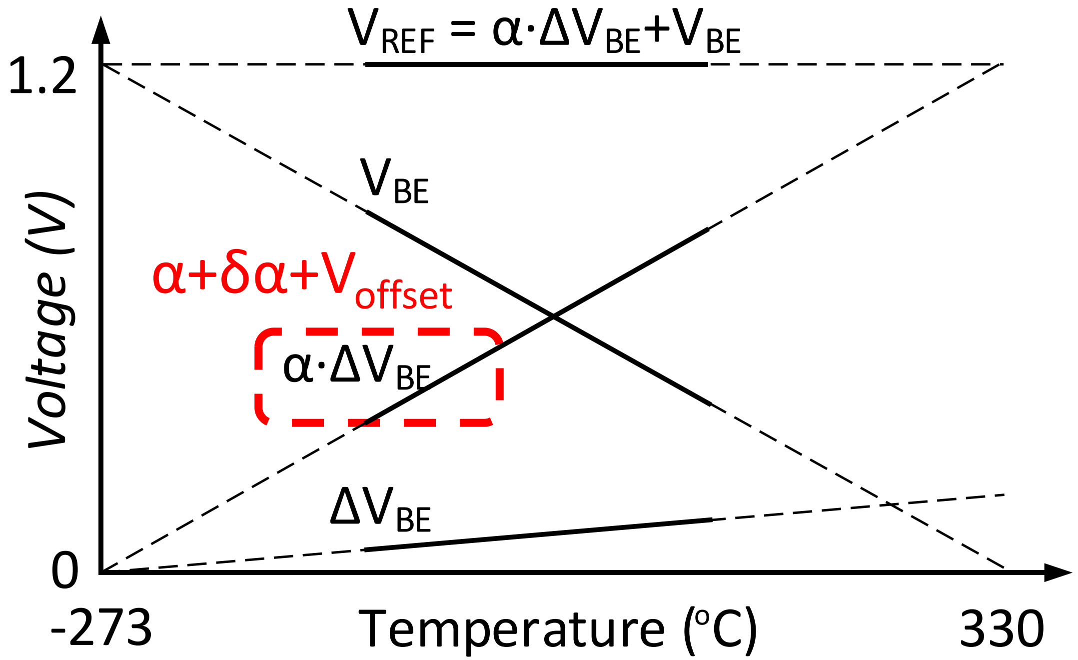

- Offset, gain error, mismatch and process spread
  - Dynamic element matching
  - Auto-zeroing/chopping
- Multiple sampling to reduce the wideband noise
- Extra errors introduced during signal conversions

Outline

- Motivation and Challenge
- Fundamentals of BJT-based CMOS Temperature Sensing
- Design Examples
  - Ultra-low Power High Accuracy CMOS Temperature Sensor for Clinical Temperature Monitoring
  - Embedded Time-Domain Wide Sensing Range CMOS Temperature Sensor
- Conclusions

Clinical Temperature Sensor

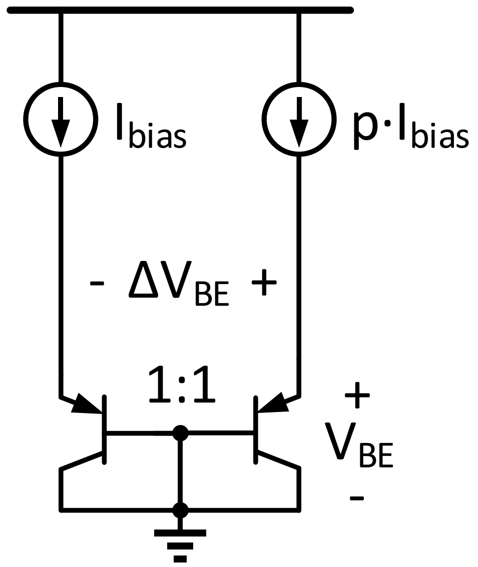

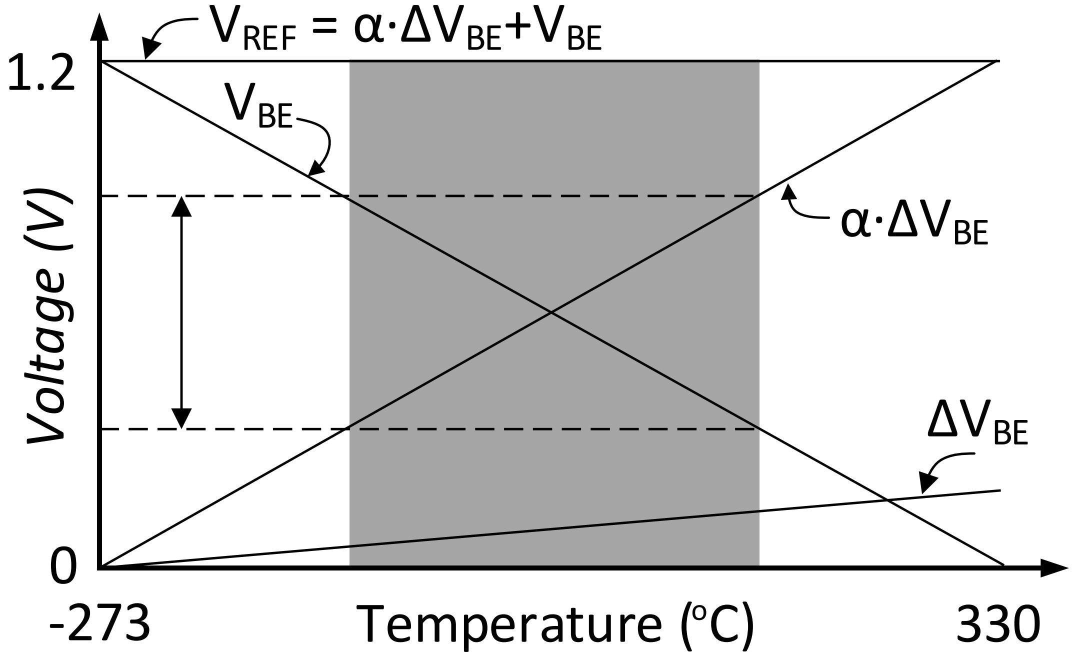

Clinical Monitoring

- ❑ Power: ~1μW
- ❑ Range: 25 ~ 45°C
- ❑ Accuracy: ±0.1°C
- ❑ Calibration: 1-point
- ❑ Rate: 1~2 Sa/s

- Input range depends on temperature range
  - Input range under-utilization for applications requiring limited sensing range (e.g. human body temperature monitoring)

Clinical Temperature Sensor

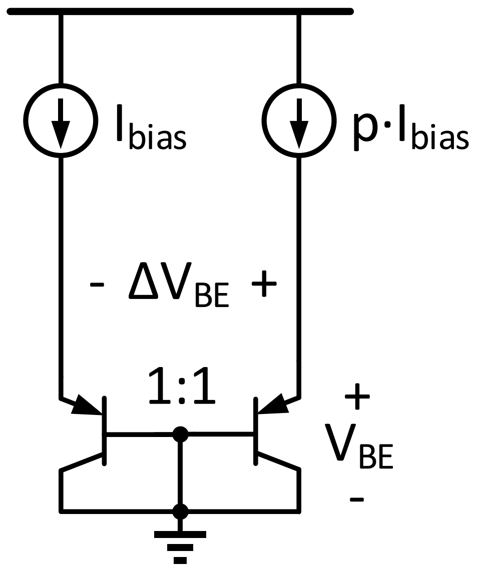

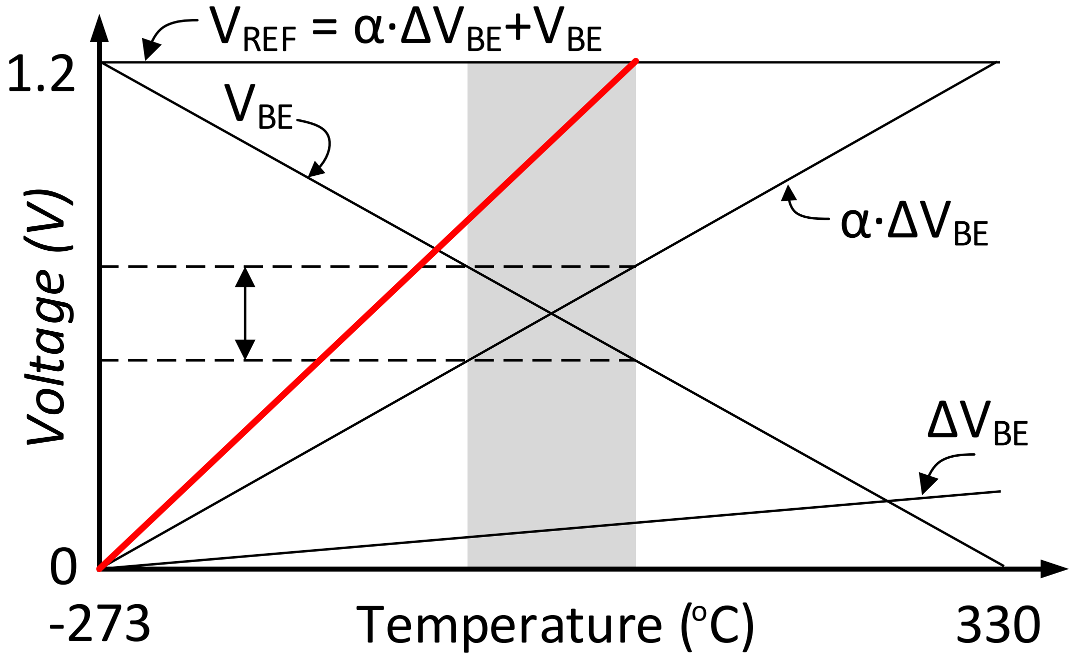

Clinical Monitoring

- ❑ Power: ~1µW
- ❑ Range: 25 ~ 45°C
- ❑ Accuracy: ±0.1°C
- ❑ Calibration: 1-point
- ❑ Rate: 1~2 Sa/s

- Input range depends on temperature range
  - Input range under-utilization for applications requiring limited sensing range (e.g. human body temperature monitoring)
- Increase temperature signal to relax ADC resolution

Clinical Temperature Sensor

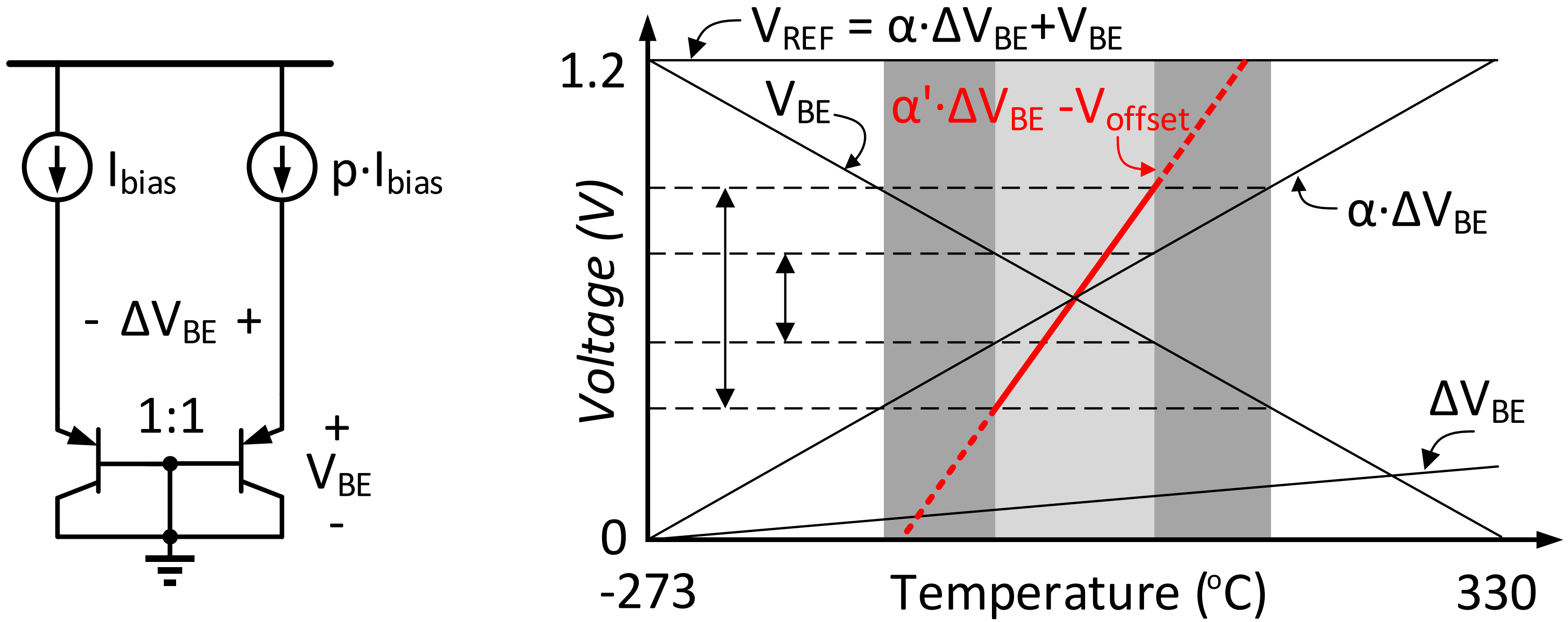

Clinical Monitoring
- ❑ Power: ~1μW
- ❑ Range: 25 ~ 45°C
- ❑ Accuracy: ±0.1°C
- ❑ Calibration: 1-point
- ❑ Rate: 1~2 Sa/s

- Input range depends on temperature range
  - Input range under-utilization for applications requiring limited sensing range (e.g. human body temperature monitoring)
- Increase temperature signal to relax ADC resolution
- Accurate gain stage (*α'*) and offset (V_{offset})

Operation Principles

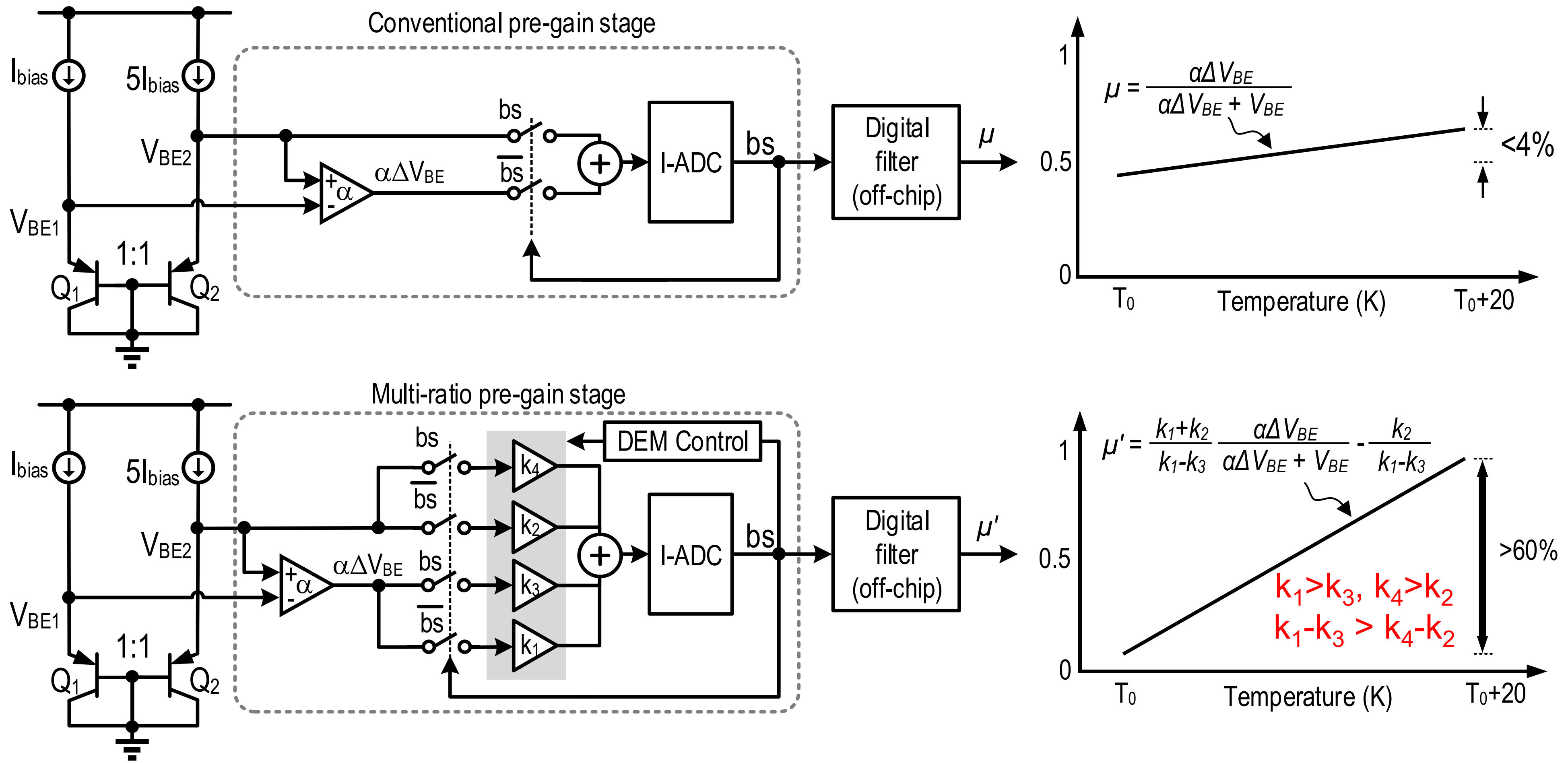

- Dynamic element matching for accurate gain/offset generation using $k_{1\text{-}4}$
- Improve ADC input range utilization from < 4% to > 60%
- Relax ADC resolution to 12-bit for 0.01°C resolution

Block-based DWA

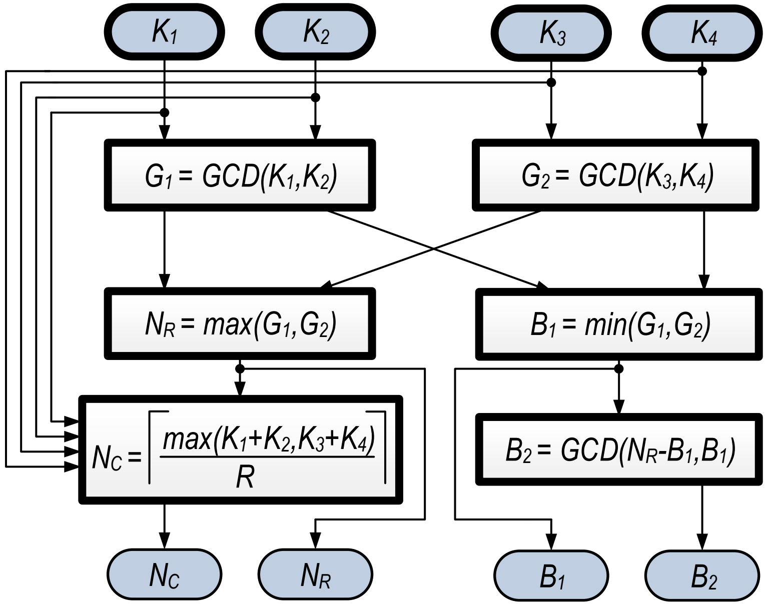

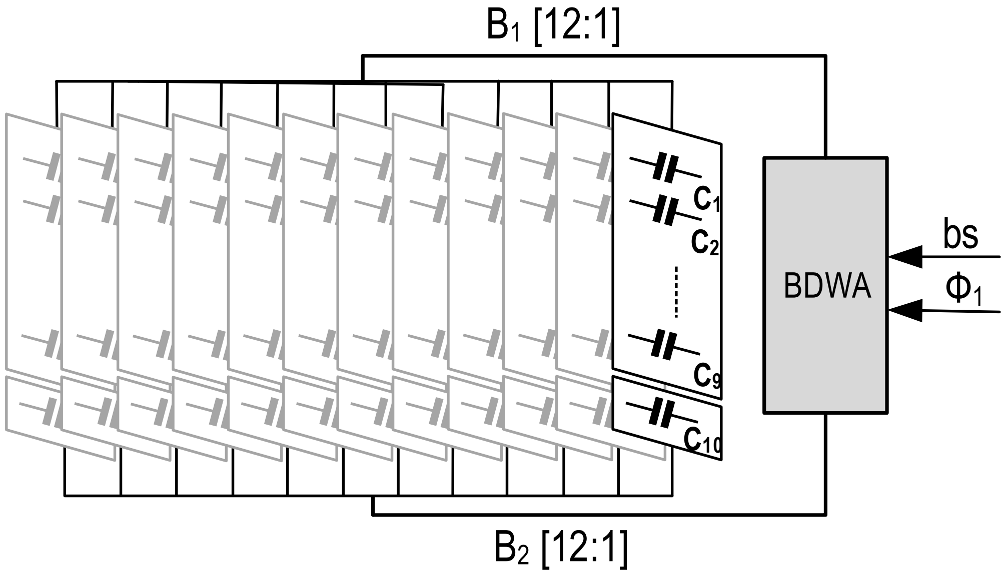

- For α = 18, $k_1 = 6$, $k_2 = 9$, $k_3 = 5$, $k_4 = 10$
  - Requires 117 unit capacitors in conventional DWA
- Blocked-based DWA
  - Group maximum number of unit capacitors into blocks while providing the flexibility offered by DWA
  - Control wiring reduce by 4.8x

System architecture

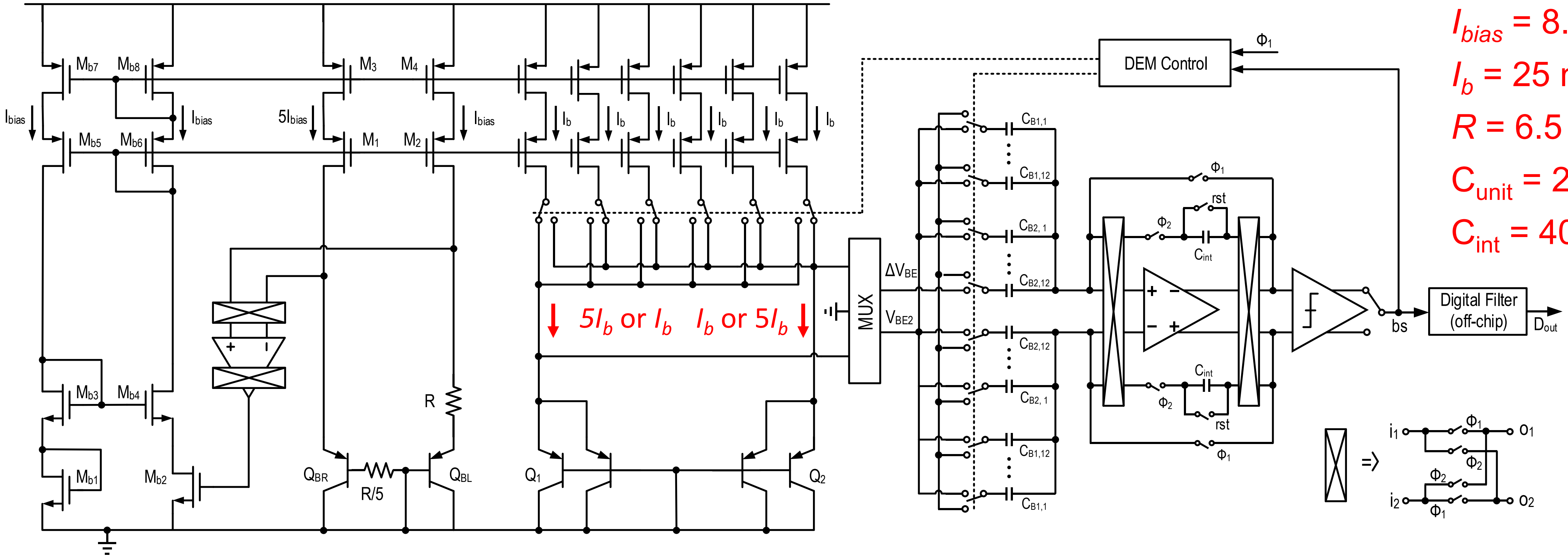

I_{bias} = 8.3 nA
I_b = 25 nA
R = 6.5 MΩ
C_{unit} = 28fF
C_{int} = 40 C_{unit}

- Dynamic Element Matching in BJT core and capacitor bank
- System level chopping to eliminate amplifier offsets
- β-compensation with R and R/5 to reduce V_{BE} non-linearity

$$I_{bias} = \frac{1+\beta_F}{\beta_F}\frac{\Delta V_{BE,RL}}{R_b} \qquad V_{BE1,2} = \frac{kT}{q} ln\left(\frac{3I_{bias}}{I_S}\frac{\beta_F}{1+\beta_F}\right) = \frac{kT}{q} ln\left(\frac{3\Delta V_{BE,RL}}{R_b I_S}\right)$$

$k_1 \cdot \alpha\Delta V_{BE} - k_2 \cdot V_{BE}$ integration (bs=0)

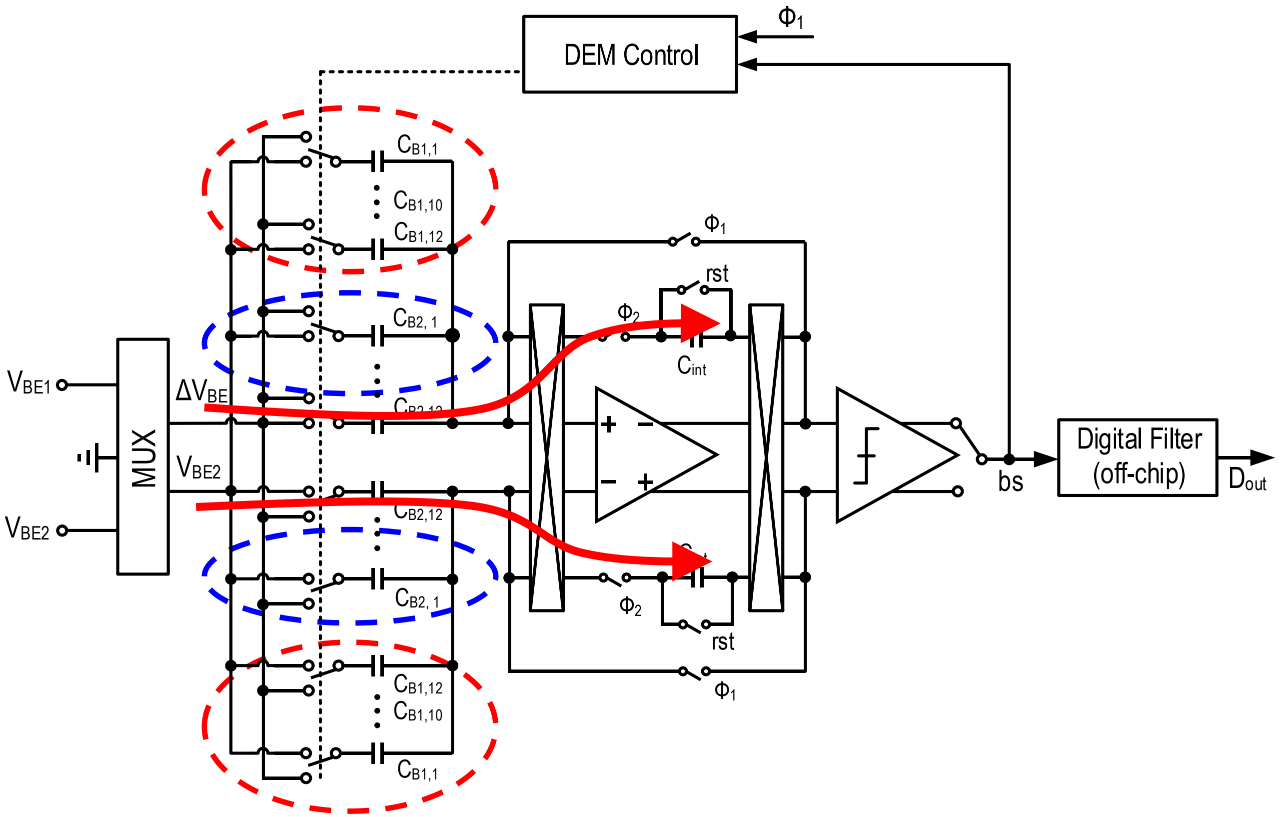

- At Φ_1 when bs=0, V_{BE} and ΔV_{BE} sampled by 9 and 108 capacitors (k_2=9, αk_1=108), together with integrator offset
- At Φ_2 when bs=0, $k_1 \cdot \alpha\Delta V_{BE} - k_2 \cdot V_{BE}$ integrated into C_{int}
- Complete in 52 cycles

$k_4 \cdot V_{BE}$ $-k_3 \cdot \alpha\Delta V_{BE}$ Integration (bs = 1)

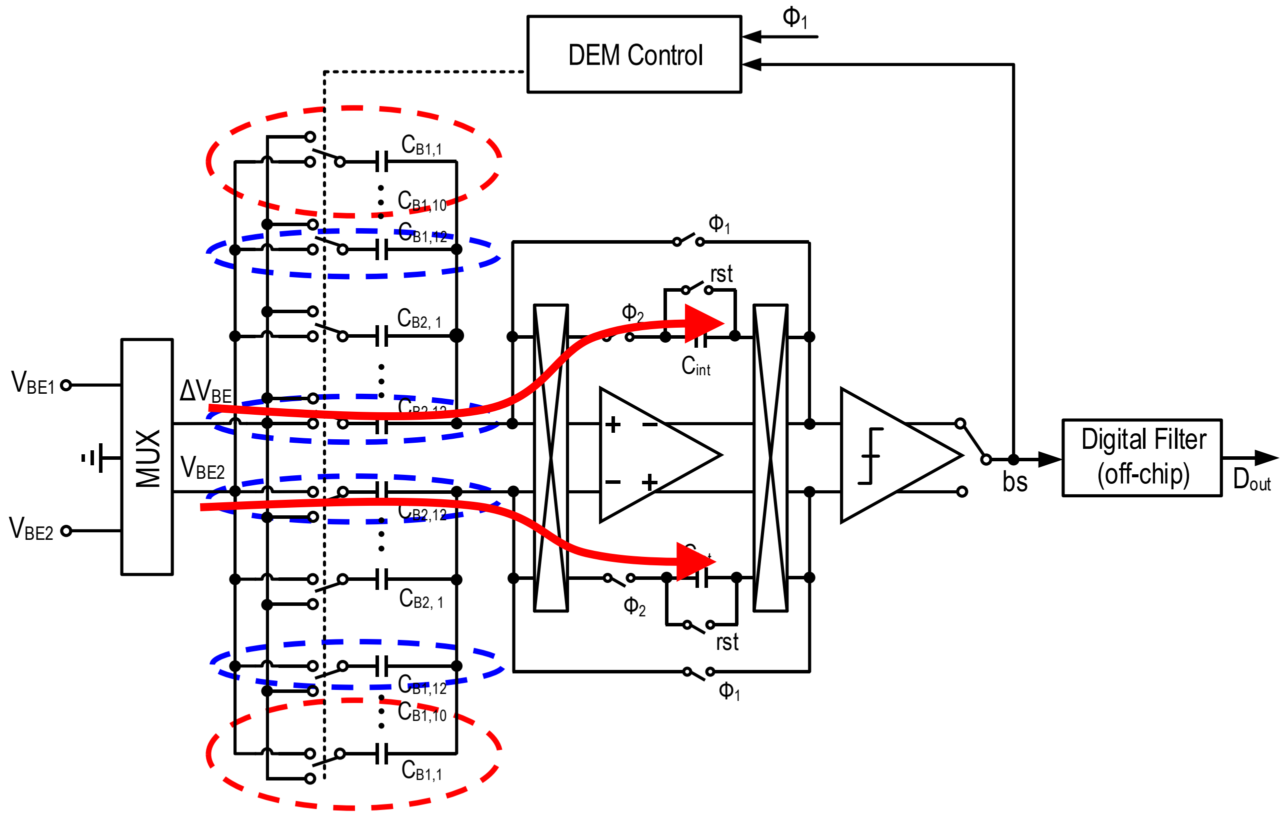

- At Φ_1 when bs=1, V_{BE} and ΔV_{BE} sampled by 10 and 90 capacitors (k_4=10, αk_3=90), together with integrator offset
- At Φ_2 when bs=1, $k_4 \cdot V_{BE} - k_3 \cdot \alpha\Delta V_{BE}$ integrated into C_{int}
- Complete in 12 cycles

Experimental Results

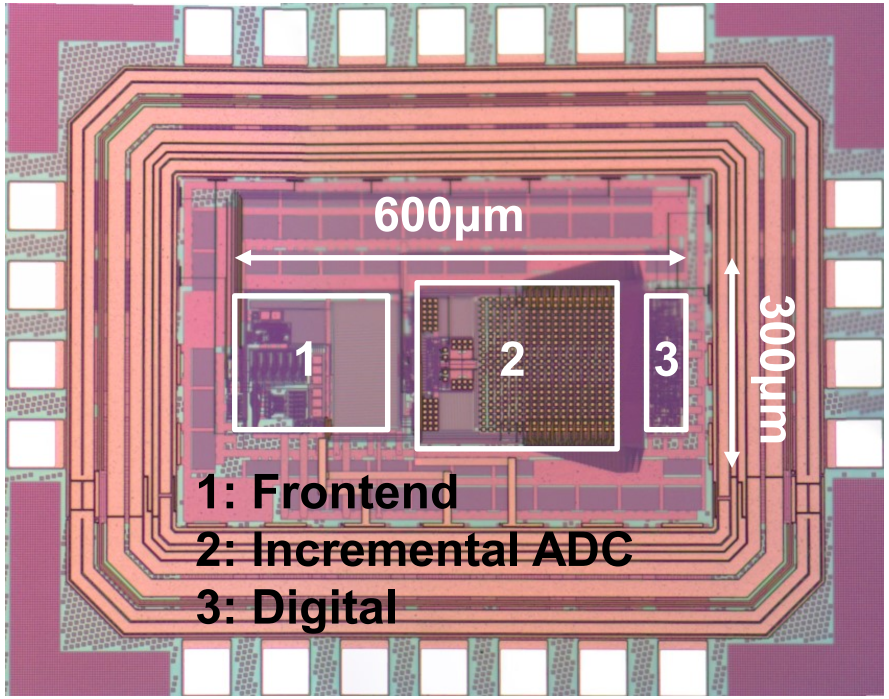

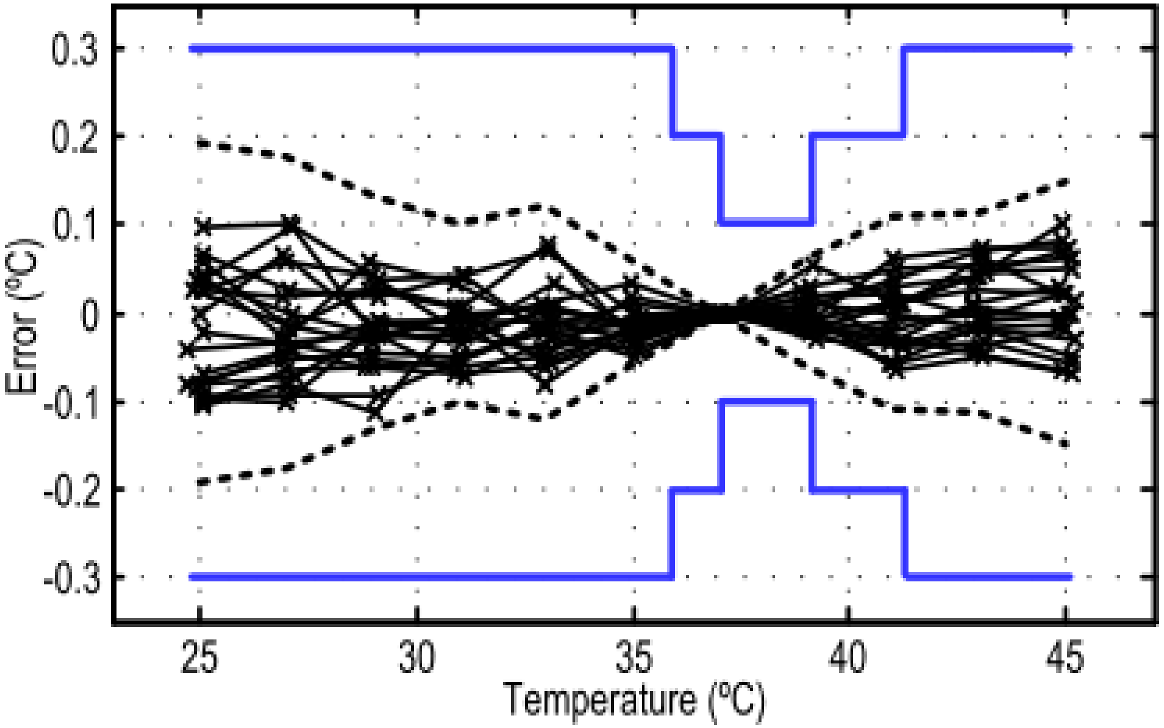

- Technology: 0.18-µm CMOS
- Power: 0.9 µW (Analog)
  0.2 µW (Digital)
- Resolution: 0.01 °C

- 20 samples from one batch
- Calibration and trimming at 37°C
- Inaccuracy (±3σ) < 0.2 °C
- Fulfill human body temperature standard

Performance Comparison

	This Work	TCAS-II'10	JSSC'10	ASSCC'07	JSSC'13	TCAS-II'17	JSSC'13
Process (µm)	**0.18**	0.35	0.18	0.18	180	0.18	0.18
Sensing Device	**BJT**	MOS	MOS	N/A	Inverters	Inverters	BJT
Sensing Range (°C)	**25~45**	35~45	-10~30	27~47	0~100	-20~80	-55~125
Inaccuracy (°C)	**±0.2***	±0.1	+1/-0.8	±1	-0.6/+3	±0.99*	±0.2*
Resolution (°C)	**0.01**	<0.035	<0.21°C	1	0.3	0.09	0.005
Power (µW)	**1.1**	0.11	0.12	0.9	0.2	0.8	5.1
Sampling rate (Sa/s)	**2**	10	333	N/A	10	1.25	10
Chip Samples	**20**	3	9	N/A	5	10	19
Calibration	**1-point**	2-point	2-point	2-point	2-point	2-point	1-point

* 3σ values from multiple chip results

Outline

- Motivation and Challenge
- Fundamentals of BJT-based CMOS Temperature Sensing
- Design Examples
  - Ultra-low Power High Accuracy CMOS Temperature Sensor for Clinical Temperature Monitoring
  - Embedded Time-Domain Wide Sensing Range CMOS Temperature Sensor
- Conclusions

Passive RFID Sense Tag

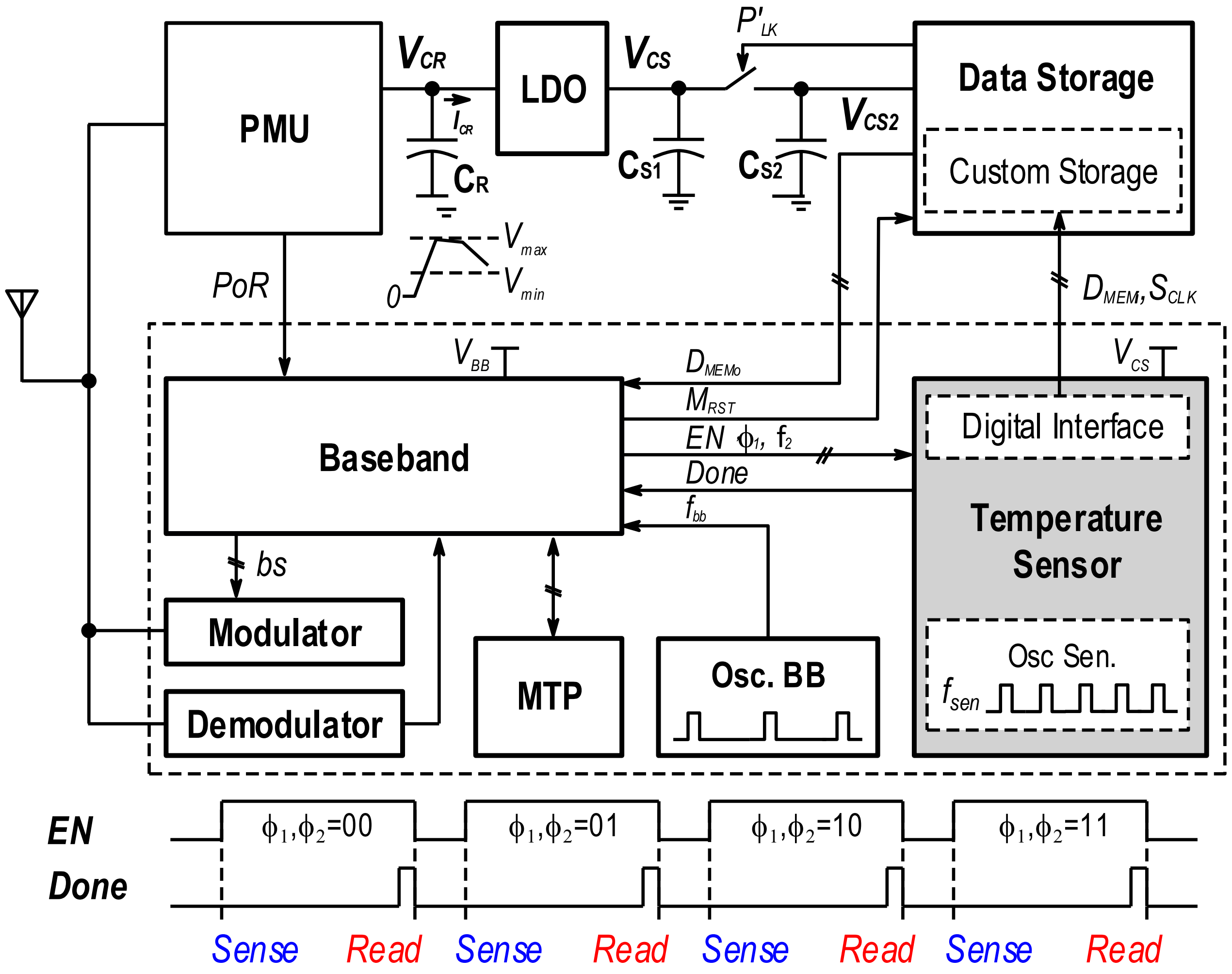

Remote Grid Monitoring

- ❑ Operating Distance: > 3m
- ❑ Power: < 3µW
- ❑ Sensing Range: -10 ~ 110^{o}C
- ❑ Accuracy: ± 2~3^{o}C
- ❑ Calibration: 1-point

- Simplified interface between different building blocks
- Custom storage cell for temporary storage of temperature sensing data

Sensor Frontend

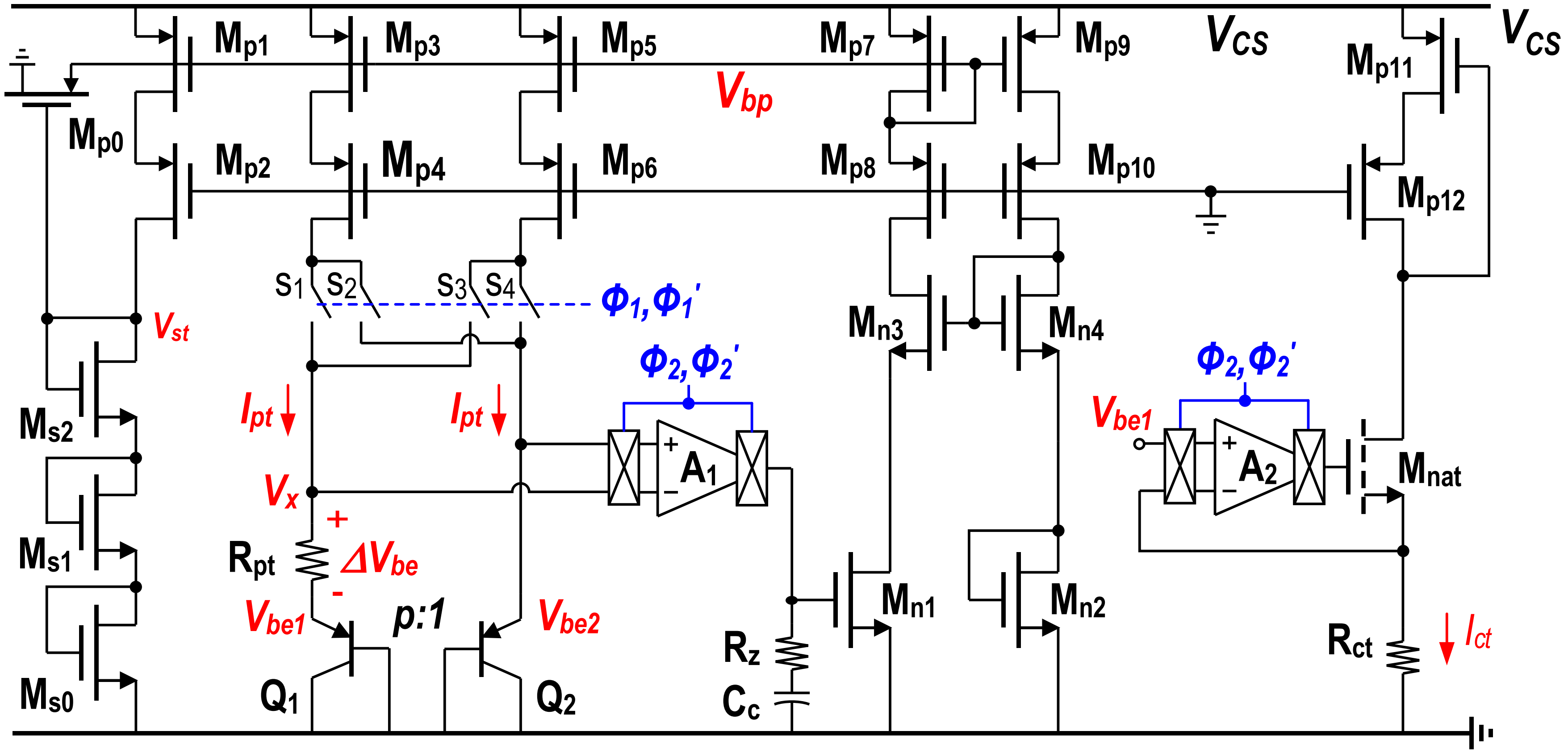

- Feedback loops for PSRR improvement
- Multiple sampling to combat RF fluctuation and mismatch errors
- Residual errors calibrated in the backend digitally
- Total 0.9 μA with V_{CS} = 1.45V

Dual-Slope Time-Domain Readout

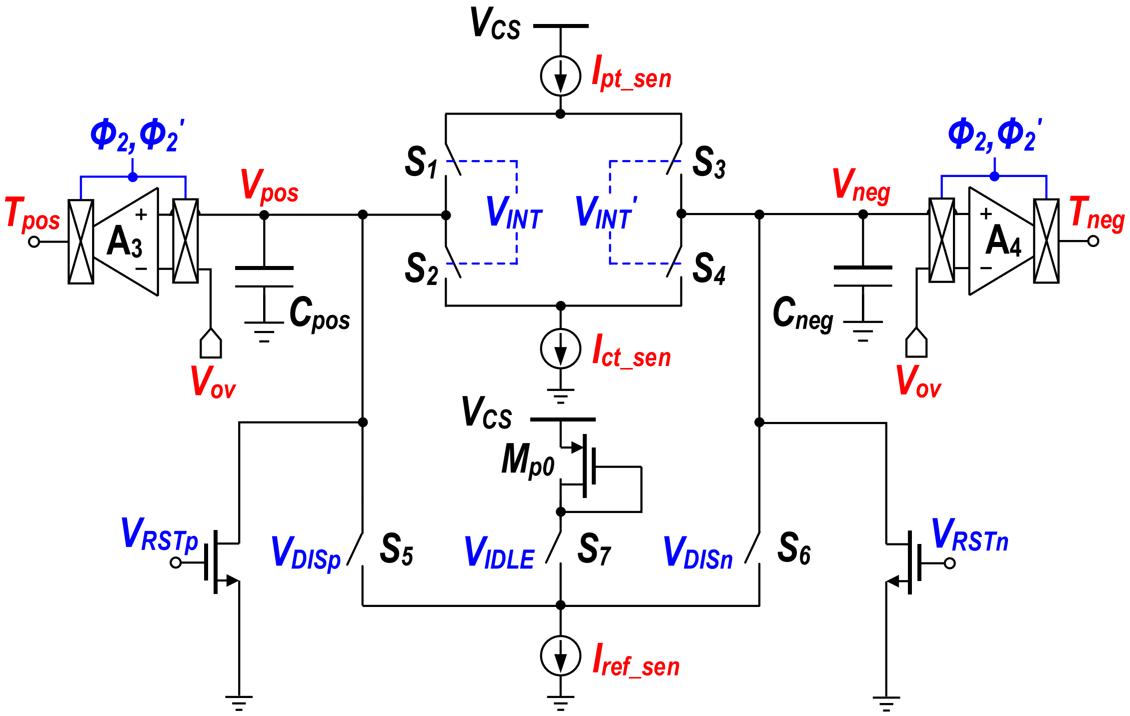

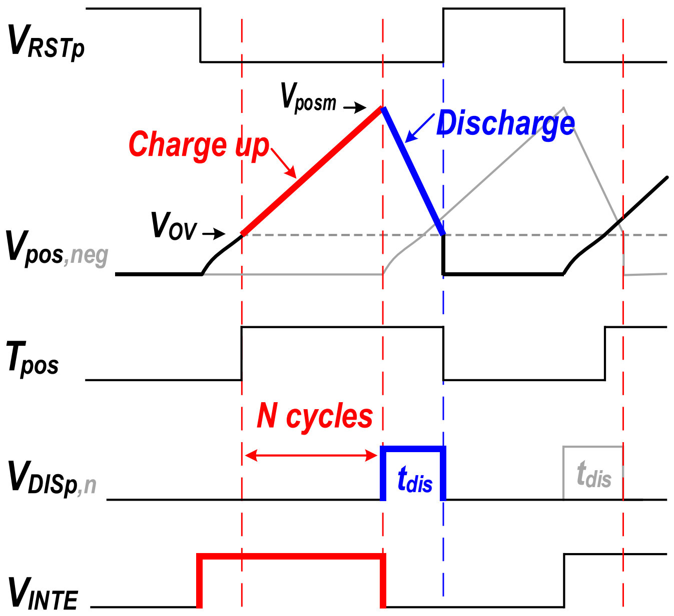

- Linear dependence between t_{dis} and f_s
- Ping-pong like operation
  - Avoid large voltage swings
  - Minimize current spikes
  - 2x conversion speed

$$\boxed{t_{dis} = \frac{N}{f_{sen}} \frac{I_{pt\_sen} - I_{ct\_sen}}{I_{ref\_sen}}}$$

Process Compensated Clock Gen.

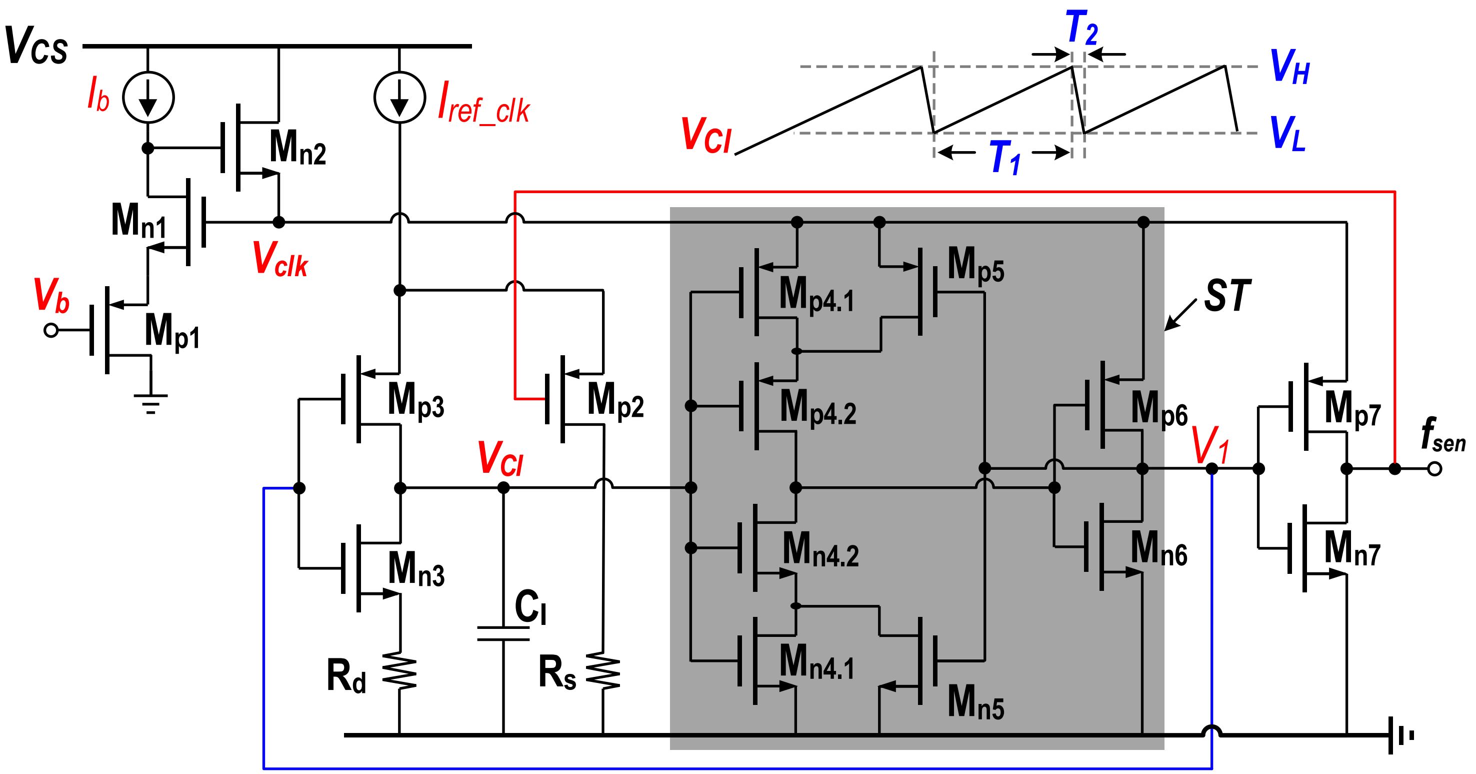

- Low power Schmitt trigger (ST): $f_{sen} \approx \frac{I_{ref\_clk}}{C_I}\frac{1}{V_H - V_L} = \frac{I_{ref\_clk}}{C_I}\frac{1}{V_{clk} - |V_{thp4}| - V_{thn4}}$
- Pseudo-supply with: $V_{clk} = |V_{thp1}| + V_{thn1} + \sqrt{2I_b/K_{p1}} + \sqrt{2I_b/K_{n1}} + V_b$
- Variation in f_{sen} reduces by >4× over PVT

Custom Low-Leakage Storage

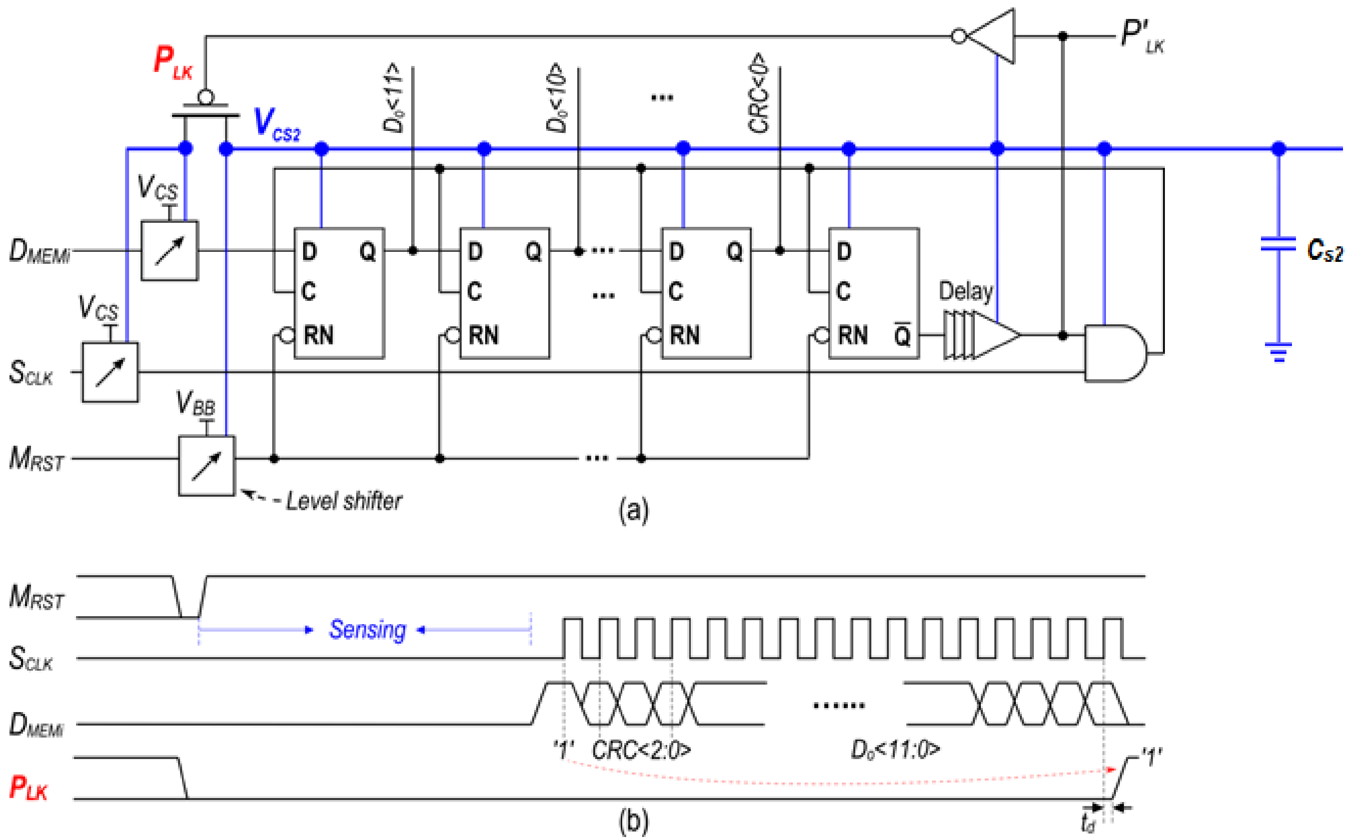

- Specific *Write* command as sensor trigger (timeout duration = 20 ms)
- All other blocks powered down to maintain a 1.4s retention time at 120^{o}C (discontinuity between write and read commands)
- CRC to ensure the data integrity

Chip Micrograph

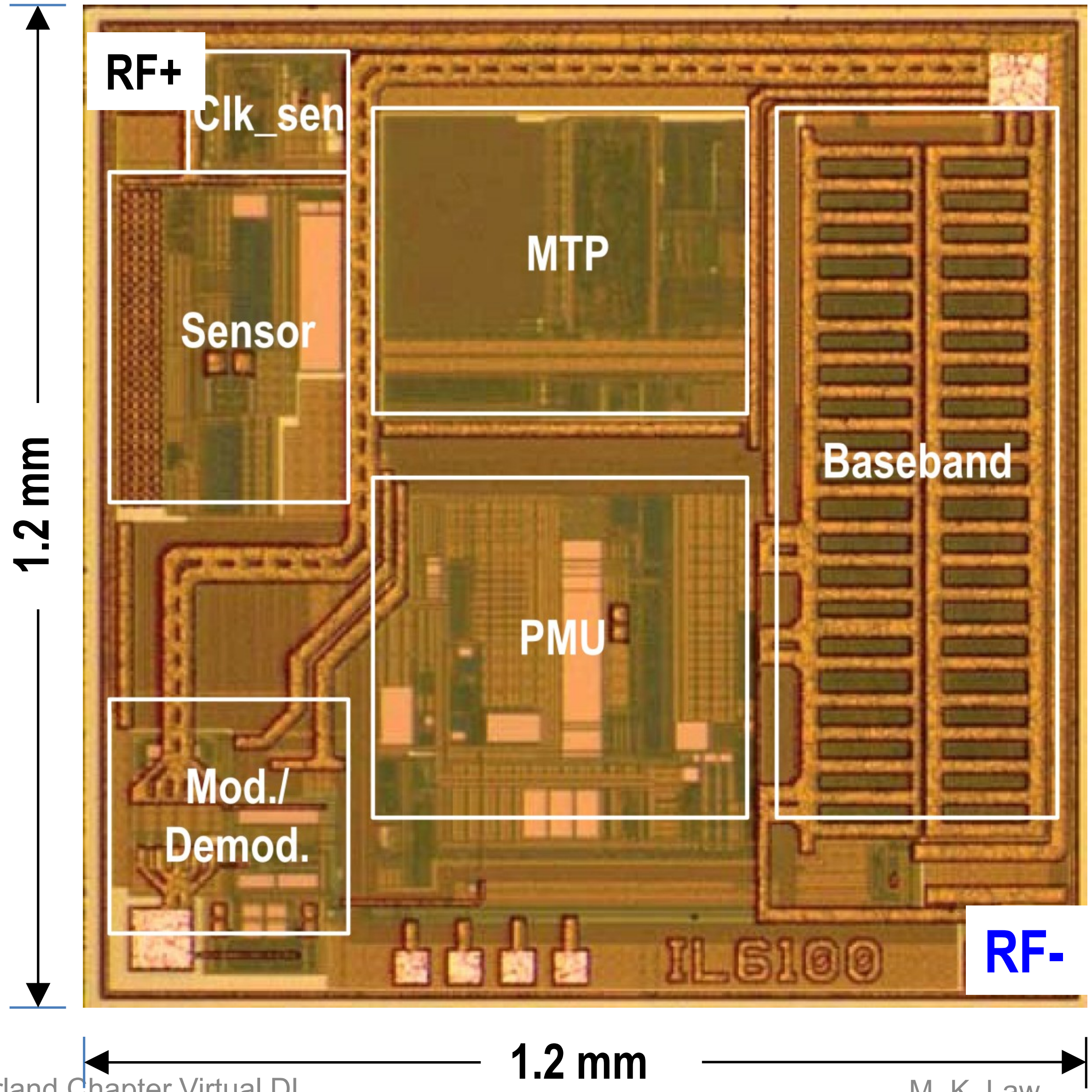

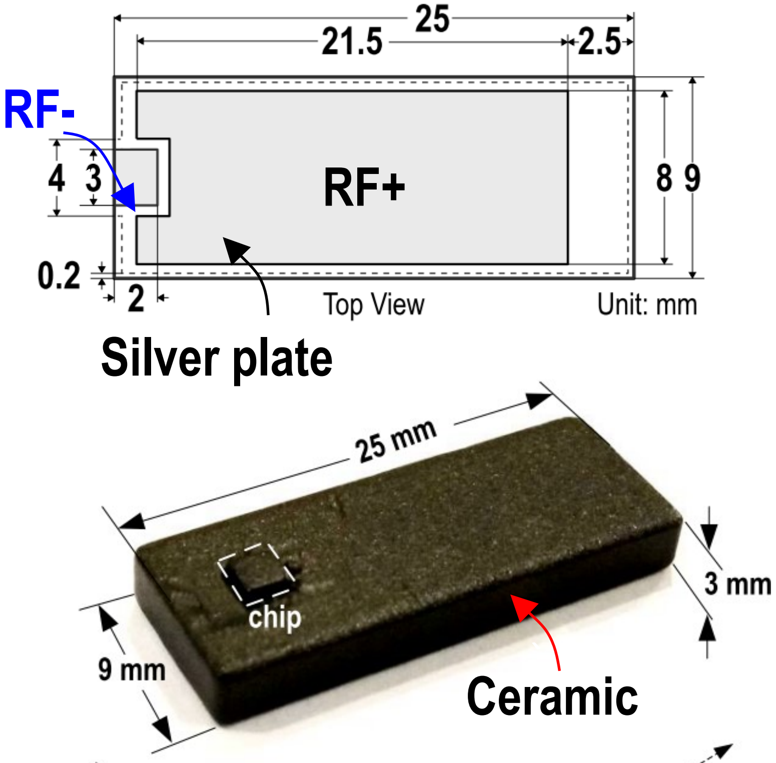

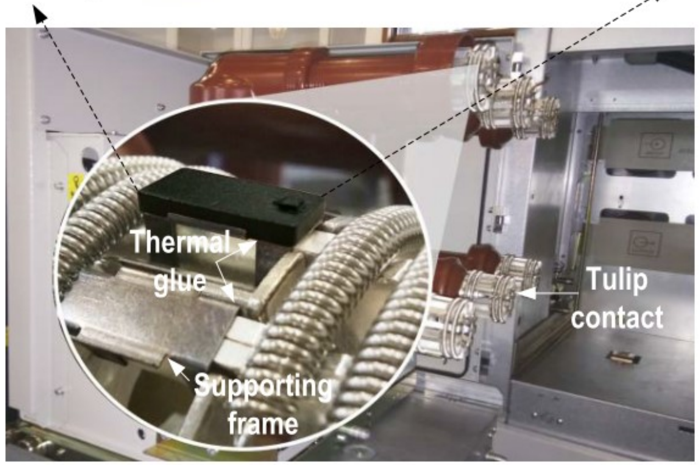

Tag Sensing Performance

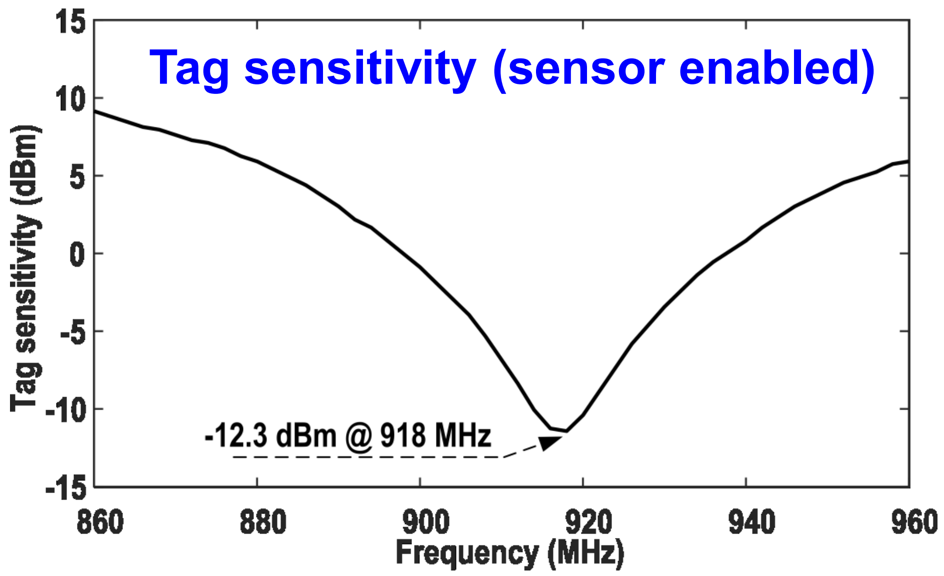

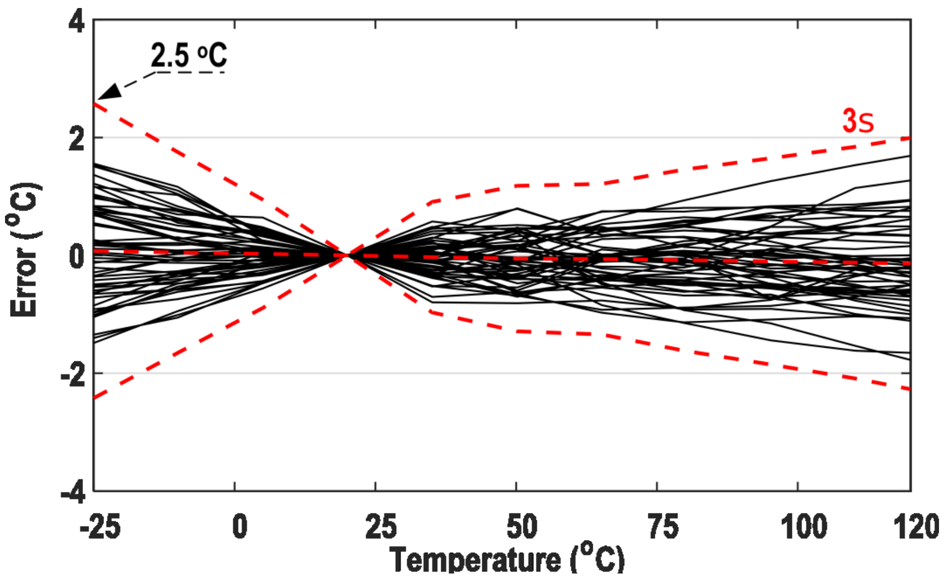

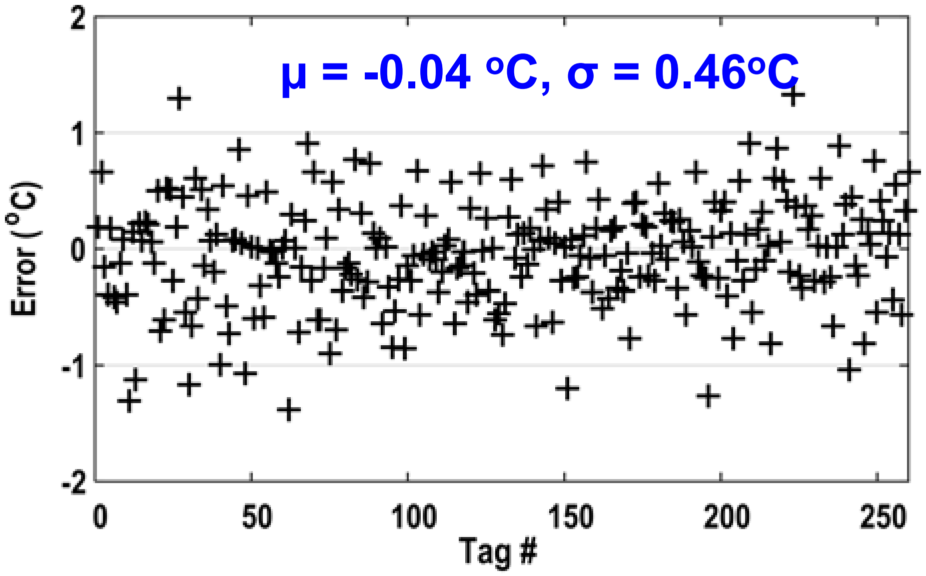

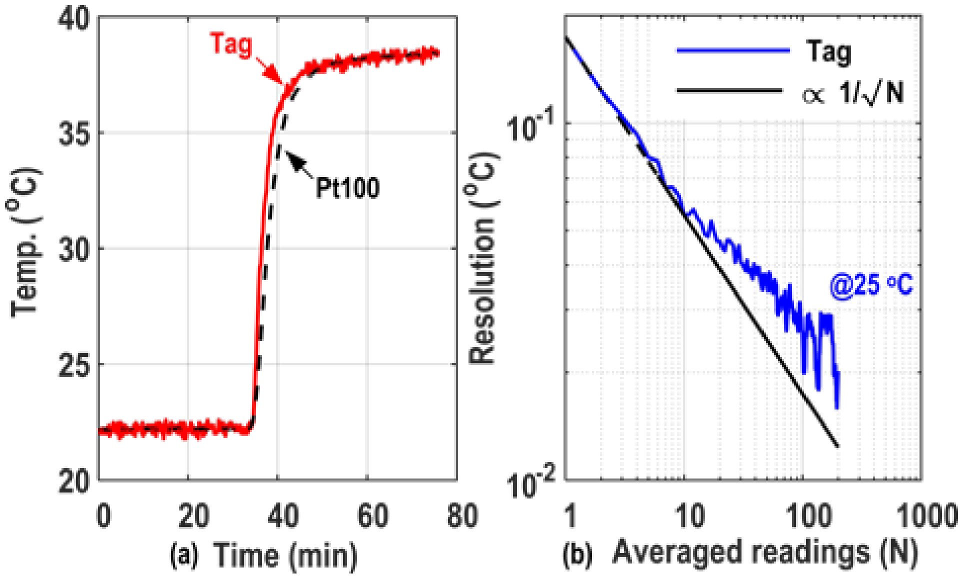

Tag Sensing Performance

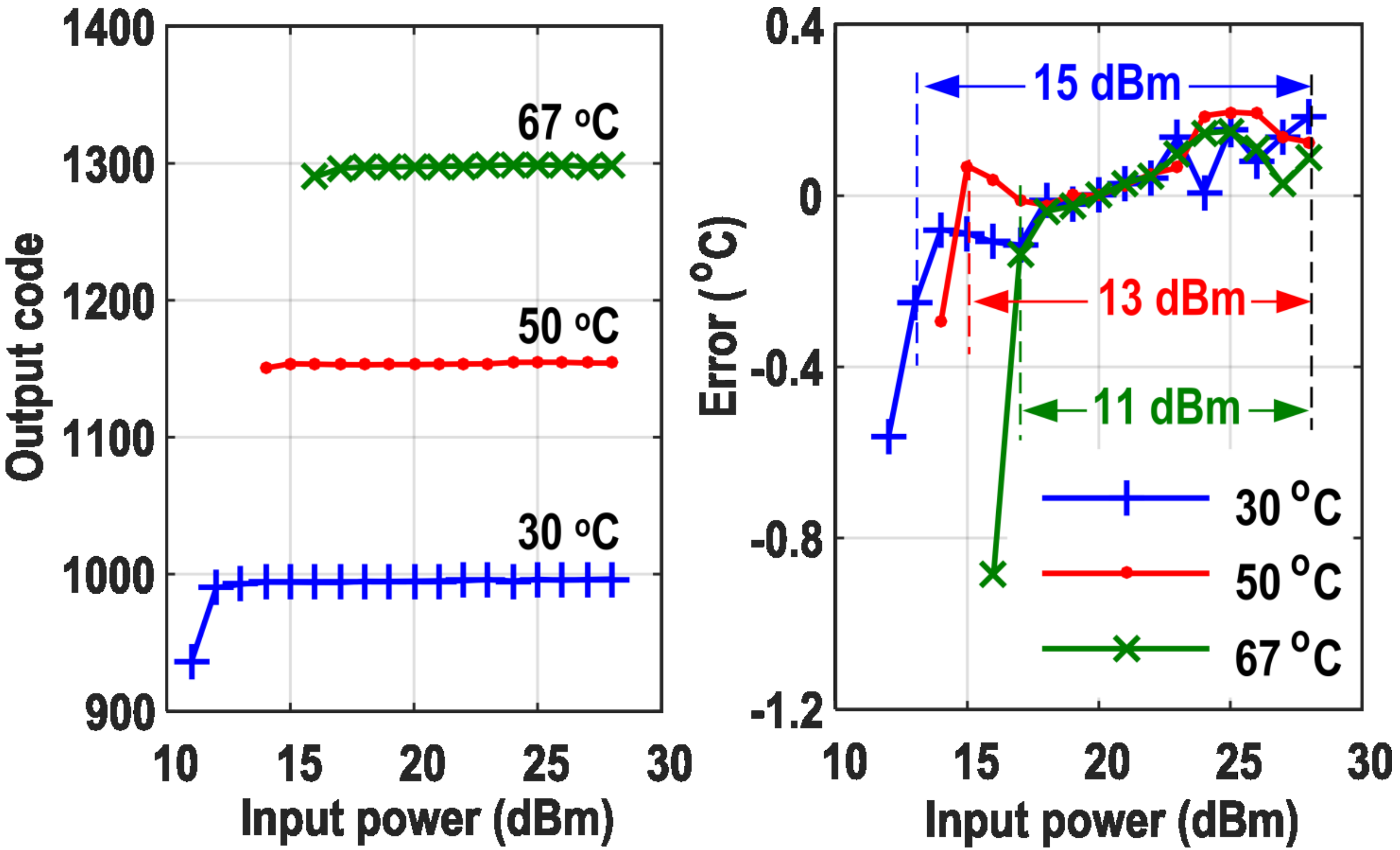

- RF power dependent error (±0.2 °C @15 dBm, 30°C)

Tag Performance Comparison

	This Work	Magnus S3	EM4325	SensTag	Electra-CT	SL900A
Type	**Passive**	Passive	Passive/BAP	Passive	Passive	Passive/BAP
Chip Area (mm^2)	**1.44**	~2.56[a]	2.95	N/A	N/A	7.14[e]
Sen. Range (°C)	**-25 ~ 120**	-40 ~ 85	-40 ~ 60	-20 ~ 105	-30 ~ 85	0 ~ 40
Sen. Acc. (°C)	**±2.5 (3σ)**	±5 / ±1	±2	±1	±0.5	±1[f]
Calibration	**1-pt**	1-pt / 2-pt	1-pt	N/A	N/A	1-pt
Rel. Acc. (%)	**3.45**	8 / 1.6	4	1.5	0.9[d]	5
Res. (°C)	**0.17**	0.25[b]	0.25	N/A	> 0.1	0.18
Chip Sen. (dBm)	**-10.8**	-9.9	-4.5	N/A	N/A	-0.7[g]
Tag Sen. (dBm)	**-12.3**	N/A	N/A	0.85[c]	-2	N/A
Sensing Dist. (m)	**3.5**	N/A	N/A	1.53	2.12	N/A

[a] Estimated from datasheet
[b] After 139 data averaging
[c] Estimated with the 5 feet reading distance, 35% rectifier efficiency and zero path loss
[d] Use 103GT-2 NTC thermistor as sensing device
[e] External sensor frontend
[f] Standalone sensing accuracy
[g] Estimated with 300μW sensing power and 35% rectifier efficiency

Outline

- Motivation and Challenge
- Fundamentals of BJT-based CMOS Temperature Sensing
- Design Examples
  - Ultra-low Power High Accuracy CMOS Temperature Sensor for Clinical Temperature Monitoring
  - Embedded Time-Domain Wide Sensing Range CMOS Temperature Sensor
- Conclusions

Conclusions

- System level considerations for embedded CMOS temperature sensor design for passive RFID tag
  - Power efficiency over energy efficiency
  - Tradeoff in accuracy/conversion time/power consumption
- BJT-based CMOS temperature sensor
  - Intrinsic errors at ultra-low power consumption
  - ADC readout for high accuracy
  - TDC readout for system level co-optimization
- High accuracy CMOS temperature sensor consuming only ~1μW
- Embedded TDC-based CMOS temperature sensor in passive RFID tag, with a nominal free space sensing distance of 3.5m with a 4W EIRP reader

Acknowledgement

- Macau FDCT under Grant 069/2016/A2
- Research Committee of University of Macau under Grant MYRG2018-AMSV-00196

References

[1] EPCglobal, “Radio-frequency identity protocols generation-2 UHF RFID air interface protocol for communications at 860 MHz-960 MHz Version 2.0.1 Ratified,” 2015.

[2] K.A.A. Makinwa, "Smart Temperature Sensors in Standard CMOS,” Procedia Engineering, pp. 930 – 939, Sept. 2010.

[3] K.A.A. Makinwa, "Smart Temperature Sensor Survey", [Online]. Available: http://ei.ewi.tudelft.nl/docs/TSensor_survey.xls

[4] R. J. Widlar, “New developments in IC voltage regulators,” IEEE J. Solid-State Circuits, vol. 6, no. 1, pp. 2–7, Feb. 1971.

[5] G. C. M. Meijer, G. Wang, F. Fruett, “Temperature Sensors and Voltage References Implemented in CMOS Technology,” IEEE Sensors J., vol. 1, no. 3, pp. 225-234, Oct. 2001.

[6] M. A. P. Pertijs, Johan H. Huijsing, Precision Temperature Sensors in CMOS Technology, The Netherlands: Springer, 2006.

[7] M. A. P. Pertijs, A. Niderkorn, X. Ma, B. McKillop, A. Bakker, J. H. Huijsing, “A CMOS smart temperature sensor with a 3σ inaccuracy of ±0.5^{o}C from -50^{o}C to 120^{o}C,” IEEE J. Solid-State Circuits, vol. 40, no. 2, pp. 454-461, Feb. 2005.

[8] W. Sansen, Analog Design Essentials, Springer US, 2006.

[9] B. Wang, M. K. Law, J. Yi, C. Y. Tsui and A. Bermak, “A -12.3 dBm Passive Sense Tag for Grid Thermal Monitoring,” IEEE Trans. on Industrial Electronics, vol. 66, no. 11, pp. 8811-8820, Nov. 2019.

[10] T. Zhang, M. K. Law, P. I. Mak, M. I Vai and R. P. Martins, “Nano-Watt Class Energy-Efficient Capacitive Sensor Interface With On-Chip Temperature Drift Compensation,” IEEE Sensors J., vol. 18, no. 7, pp. 2870-2882, Apr. 2018.

[11] B. Wang, M. K. Law, C. Y. Tsui and A. Bermak, “A 10.6 pJ·K^2 Resolution FoM Temperature Sensor Using Astable Multivibrator,” IEEE Trans. on Circuits Syst. II, Exp. Briefs, vol. 65, no. 7, pp. 869-873, Jul. 2018.

[12] M. K. Law, S. Lu, T. Wu, A. Bermak, P. I. Mak and R. P. Martins, “A 1.1 μW CMOS Smart Temperature Sensor with an Inaccuracy of ±0.2oC (3σ) for Clinical Temperature Monitoring,” IEEE Sensors J., vol. 16, no. 8, pp. 2272-2281, Feb. 2016.

[13] B. Wang, M. K. Law, A. Bermak and H. C. Luong, “A Passive RFID Tag Embedded Temperature Sensor With Improved Process Spreads Immunity for a -30℃ to 60℃ Sensing Range”, IEEE Trans. on Circuits and Systems I, vol. 61, no. 2, pp. 337 – 346, Feb. 2014.

[14] J. Yin, J. Yi, M. K. Law, Y. Ling, M. C. Lee, K. P. Ng, B. Gao, H. C. Luong, A. Bermak, M. Chan, W. H. Ki, C. Y. Tsui and M. Yuen, "A system-on-chip EPC Gen-2 passive UHF RFID tag with embedded temperature sensor," IEEE J. Solid-State Circuits, vol. 45, no. 11, pp. 2404-2420, Nov. 2010.

[15] M. K. Law, A. Bermak, H. C. Luong, “A Sub-μW Embedded CMOS Temperature Sensor for RFID Food Monitoring,” IEEE J. Solid-State Circuits, vol. 45, no. 6, pp. 1246-1255, Jun. 2010.

[16] M. K. Law, A. Bermak, “A 405-nW CMOS temperature sensor based on linear MOS operation,” IEEE Trans. Circuits Systs. II, Exp. Briefs, vol. 56, no. 12, pp. 891-895, Dec. 2009.

Thank you for your attention.